REPORT DOCUMENTATION PAGE

AFRL-SR-BL-TR-99-

0117

1. AGENCY USE ONLY *(Leave blank)*	2. REPORT DATE	3. REPORT TYPE AND DATES COVERED
		Final 01 Apr 97 to 31 Dec 98

4. TITLE AND SUBTITLE
LARGE-EDDY SIMULATION OF THE FLOW OVER A LOW-REYNOLDS NUMBER AIR FOIL

5. FUNDING NUMBERS
61102F
2304/KV

6. AUTHOR(S)
PROFESSOR PIOMELLI

7. PERFORMING ORGANIZATION NAME(S) AND ADDRESS(ES)
UNIVERSITY OF MARYLAND
2100 LEE BUILDING
COLLEGE PARK MD 20742-5141

8. PERFORMING ORGANIZATION REPORT NUMBER

9. SPONSORING/MONITORING AGENCY NAME(S) AND ADDRESS(ES)
AFOSR/NM
801 NORTH RANDOLPH STREET RM 732
ARLINGTON, VA 22203

10. SPONSORING/MONITORING AGENCY REPORT NUMBER
F49620-97-1-0244

11. SUPPLEMENTARY NOTES

12a. DISTRIBUTION AVAILABILITY STATEMENT
APPROVAL FOR PUBLIC RELEASED; DISTRIBUTION UNLIMITED

12b. DISTRIBUTION CODE

13. ABSTRACT *(Maximum 200 words)*

An a priori study of subgrid-scale models for the unclosed terms in the energy equation is carried out using the flow field obtained from the direct simulation of homogeneous isotropic turbulence. Scale-similar models involve multiple filtering operations to identify the smallest resolved scales and have been shown to be the most active in the interaction with the unresolved subgrid scales (SGS). In the present study these models are found to give more accurate prediction of the SGS stresses and heat fluxes than eddy-viscosity and eddy-diffusivity models, as well as improve prediction of the SGS turbulent diffusion. SGS viscous dissipation, and SGS viscous diffusion.

14. SUBJECT TERMS			15. NUMBER OF PAGES
			16. PRICE CODE
17. SECURITY CLASSIFICATION OF REPORT	**18. SECURITY CLASSIFICATION OF THIS PAGE**	**19. SECURITY CLASSIFICATION OF ABSTRACT**	**20. LIMITATION OF ABSTRACT**
UNCLASSIFIED	UNCLASSIFIED	UNCLASSIFIED	UL

LARGE EDDY SIMULATION OF THE FLOW OVER A LOW REYNOLDS-NUMBER AIRFOIL

Final report

Ugo Piomelli
Dept. of Mechanical Engineering
University of Maryland
College Park

During the grant period, April 1, 1997–December 31, 1998, the following tasks were accomplished:

1. Model development

An *a priori* study of subgrid-scale models for the unclosed terms in the energy equation has been carried out using the flow field obtained from the direct simulation of homogeneous isotropic turbulence. Scale-similar models involve multiple filtering operations to identify the smallest resolved scales that have been shown to be the most active in the interaction with the unresolved subgrid scales (SGS). These models were found to give more accurate prediction of the SGS stresses and heat fluxes than eddy-viscosity and eddy-diffusivity models, as well as improve prediction of the SGS turbulent diffusion, SGS viscous dissipation, and SGS viscous diffusion. The turbulent diffusion term has, in the past, been neglected, or modeled heuristically. The present work examined this term rationally for the first time. The model proposed is inexpensive (since it does not require the calculation of additional terms, but is based on the model fo the SGS stresses themselves), and gives good results in the *a priori* tests carried out so far.

This work has resulted in a paper accepted at the *3rd ASME/JSME Joint Fluids Engineering Conference*, which was subsequently expanded and submitted to *Theoretical and Computational Fluid Dynamics*. The two papers are enclosed.

2. Boundary-layer calculations

Time-developing turbulent boundary layers over an isothermal flat plate at free-stream Mach numbers of 0.3 and 0.7 have been computed using an explicit finite-difference method on structured multi-block grids. The size of each block is adjusted depending on the dimension of the largest structures present locally in the flow. This results in substantial savings of memory and CPU time, compared to standard single-block methods. In the calculations presented the near-wall region is computed using a domain with a spanwise length $L_o^+ = 820$, which is sufficient to contain several streaks. This grid block is repeated periodically in the spanwise direction. The outer layer, which contains larger structures, is computed using a domain that is twice as wide ($L_o^+ = 1640$). Although the flow at the interface between the blocks has a periodicity length determined by the inner-layer block, within a few grid points

longer wavelengths are generated by the non-linear interactions. The velocity statistics and rms intensities compare well with single-block calculations that use substantially more grid points.

The advantage of this method is that, for flows that are homogeneous in one direction, it makes the cost of the calculation nearly independent of the Reynolds number, without requiring additional modeling of the wall layer. Flows of this type include airfoils, axisymmetric combustors, and other two-dimensional or axisymmetric configurations.

This work has resulted in a paper that has been submitted to the *Journal of Computational Physics*, and that will also be presented at the *Second Air Force International Direct and Large-eddy Simulation Conference.* The paper is enclosed.

Proceedings of the
3rd ASME/JSME Joint Fluids Engineering Conference
July 18–23, 1999, San Francisco, California, USA

FEDSM 99-7313

A PRIORI TESTS OF SGS MODELS IN COMPRESSIBLE TURBULENCE

M. Pino Martín
Dept. of Aero. Eng. and Mechanics
University of Minnesota
Minneapolis, MN 55455
Email: pino@aem.umn.edu

Ugo Piomelli*
Dept. of Mechanical Engineering
University of Maryland
College Park, MD 20742
Email: ugo@eng.umd.edu

Graham V. Candler
Dept. of Aero. Eng. and Mechanics
University of Minnesota
Minneapolis, MN 55455
Email: candler@aem.umn.edu

ABSTRACT

An *a priori* study of subgrid-scale models for the unclosed terms in the energy equation is carried out using the flow field obtained from the direct simulation of homogeneous isotropic turbulence. Scale-similar models involve multiple filtering operations to identify the smallest resolved scales and have been shown to be the most active in the interaction with the unresolved subgrid scales (SGS). In the present study these models are found to give more accurate prediction of the SGS stresses and heat fluxes than eddy-viscosity and eddy-diffusivity models, as well as improve prediction of the SGS turbulent diffusion, SGS viscous dissipation, and SGS viscous diffusion.

1 Introduction

Large-eddy simulation (LES) is a technique intermediate between the direct simulation (DNS) of turbulent flows and the solution of the Reynolds-averaged equations. In LES the contribution of the large, energy-carrying structures to momentum and energy transfer is computed accurately, and only the effect of the smallest scales of turbulence is modeled. Since the small scales tend to be more homogeneous and universal, and less affected by the boundary conditions than the large ones, there is hope that their models can be simpler and require fewer adjustments when applied to different flows than similar models for the Reynolds-averaged Navier-Stokes equations.

While a substantial amount of research has been carried out into the modeling aspects and requirements for incompressible flows, the applications of large-eddy simulation to compressible flows have been significantly fewer. One of the reasons for the comparatively small number of calculations of compressible flows is undoubtedly the additional complexity introduced by the need to solve an energy equation, which introduces extra unclosed terms. In addition to the subgrid scale stresses that must be modeled in incompressible flows as well, several other unclosed terms appear in the filtered equations for compressible flows. Furthermore, the form of the unclosed terms depends on the form of the energy equation chosen (internal or total energy, total energy of the resolved field or enthalpy).

Early applications of LES to compressible flows used a transport equation for the internal energy per unit mass, ε (Moin *et al.* 1991, El-Hady *et al.* 1994) or for the enthalpy per unit mass, h (Speziale *et al.* 1988, Erlebacher *et al.* 1992). In these equations, the SGS heat flux was modeled in a manner similar to that used for the SGS stresses, and the remaining terms (the SGS pressure-dilatation Π_{dil}, and the SGS contribution to the viscous dissipation, ε_v) were neglected.

Vreman *et al.* (1995b) performed *a priori* tests using DNS data obtained from the calculation of a mixing layer at Mach numbers in the range 0.2–0.6 to establish the validity of these assumptions. They found that the SGS pressure-dilatation and SGS viscous dissipation are of the same order as the divergence of the SGS heat flux Q_j, and that modeling ε_v improves the results, especially at moderate or high Mach numbers.

Vreman *et al.* (1995a,1995b) proposed the use of a transport equation for the total energy of the filtered field, rather than either the enthalpy or the internal energy equations; the same unclosed terms that appear in this equation are also present in the internal energy and enthalpy equations. This equation was also used by

*Address all correspondence to this author.

Normand and Lesieur (1992), who neglected both Π_{dil} and ε_v.

Very few calculations have been carried out using the transport equation for the total energy, despite the desirable feature that it is a conserved quantity, and that all the SGS terms in this equation can be cast in conservative form. This equation has a completely different set of unclosed terms, whose modeling is not very advanced yet. Knight *et al.* (1998) performed the LES of isotropic homogeneous turbulence on unstructured grids and compared the results obtained with the Smagorinsky (1963) model with those obtained when the energy dissipation was provided only by the dissipation inherent in the numerical algorithm. They modeled the SGS heat flux and an SGS turbulent diffusion term, and neglected the SGS viscous diffusion.

In this paper, the flow field from a DNS of homogeneous isotropic turbulence is used to compute the terms in the energy equations, and evaluate possible models for their parameterization. The work will be focused mainly in the total energy equation, both because of the lack of previous studies of the terms that appear in it, and because of the desirability of solving a transport equation for a conserved quantity.

In the following section, the governing equations are presented, the terms that require closure are defined, and the DNS database used for the *a priori* tests is described. In Sections 3 and 4 several models for the unclosed terms are presented and tested. Finally, some conclusions are drawn in Section 5.

2 Problem formulation

2.1 Governing equations

To separate the large from the small scales, LES is based on the definition of a filtering operation: a filtered (or resolved, or large-scale) variable, denoted by an overbar, is defined as (Leonard 1974)

$$\overline{f}(\mathbf{x}) = \int_D f(\mathbf{x}')G(\mathbf{x},\mathbf{x}';\overline{\Delta})d\mathbf{x}', \tag{1}$$

where D is the entire domain and G is the filter function, and $\overline{\Delta}$ is the filter width, *i.e.*, the wavelength of the smallest scale retained by the filtering operation. The filter function determines the size and structure of the small scales.

In compressible flows, it is convenient to use Favre-filtering (Favre 1965a, 1965b) to avoid the introduction of subgrid-scale terms in the equation of conservation of mass. A Favre-filtered variable is defined as:

$$\tilde{f} = \overline{\rho f}/\overline{\rho}. \tag{2}$$

To obtain the equations governing the motion of the resolved eddies, the Favre-filtering operation must be applied to the equations of conservation of mass, momentum and energy. In compressible flows, in addition to the mass and momentum equations, one can choose between solving an equation for the internal energy, enthalpy or total energy. The filtered equations of motion, then, can be put in the form:

$$\frac{\partial\overline{\rho}}{\partial t} + \frac{\partial}{\partial x_j}(\overline{\rho}\,\widetilde{u}_j) = 0, \tag{3}$$

$$\frac{\partial\overline{\rho}\,\widetilde{u}_i}{\partial t} + \frac{\partial}{\partial x_j}(\overline{\rho}\,\widetilde{u}_i\widetilde{u}_j + \overline{p} - \widetilde{\sigma}_{ji}) = -\frac{\partial\tau_{ji}}{\partial x_j} \tag{4}$$

$$\frac{\partial(\overline{\rho}\,\widetilde{\varepsilon})}{\partial t} + \frac{\partial}{\partial x_j}(\overline{\rho}\,\widetilde{u}_j\widetilde{\varepsilon}) + \frac{\partial\widetilde{q}_j}{\partial x_j} + \overline{p}\widetilde{S}_{kk} - \widetilde{\sigma}_{ji}\widetilde{S}_{ij} = -C_v\frac{\partial Q_j}{\partial x_j} - \Pi_{dil} + \varepsilon_v, \tag{5}$$

$$\frac{\partial(\overline{\rho}\,\widetilde{h})}{\partial t} + \frac{\partial}{\partial x_j}\left(\overline{\rho}\,\widetilde{u}_j\widetilde{h}\right) + \frac{\partial\widetilde{q}_j}{\partial x_j} - \frac{\partial\overline{p}}{\partial t} - \widetilde{u}_j\frac{\partial\overline{p}}{\partial x_j} - \widetilde{\sigma}_{ji}\widetilde{S}_{ij} = -C_v\frac{\partial Q_j}{\partial x_j} - \Pi_{dil} + \varepsilon_v, \tag{6}$$

$$\frac{\partial}{\partial t}(\overline{\rho}\,\widetilde{E}) + \frac{\partial}{\partial x_j}\left[(\overline{\rho}\,\widetilde{E} + \overline{p})\widetilde{u}_j + \widetilde{q}_j - \widetilde{\sigma}_{ji}\widetilde{u}_j\right] = -\frac{\partial}{\partial x_j}\left(\gamma C_v Q_j + \frac{1}{2}\mathcal{J}_j - \mathcal{D}_j\right). \tag{7}$$

Here, u_j is the velocity in the j direction, ρ is the density, p the pressure and T the temperature, $\varepsilon = c_v T$ is the internal energy per unit mass, $h = \varepsilon + p/\rho$ is the enthalpy per unit mass, $E = \varepsilon + u_i u_i/2$ is the total energy per unit mass, and the diffusive fluxes are given by

$$\widetilde{\sigma}_{ij} = 2\widetilde{\mu}\widetilde{S}_{ij} - \frac{2}{3}\widetilde{\mu}\delta_{ij}\widetilde{S}_{kk}, \qquad \widetilde{q}_j = -\widetilde{k}\frac{\partial\widetilde{T}}{\partial x_j}, \tag{8}$$

where $\widetilde{\mu}$ is the molecular viscosity, and $\widetilde{k}$ is the thermal conductivity corresponding to the filtered temperature $\widetilde{T}$. The effect of the subgrid scales appears through the SGS stresses τ_{ij}, the SGS heat flux Q_j, the SGS pressure-dilatation Π_{dil}, the SGS contribution to the viscous dissipation, ε_v, the SGS turbulent diffusion $\partial\mathcal{J}_j/\partial x_j$, and the SGS contribution to viscous diffusion, $\partial\mathcal{D}_j/\partial x_j$; these quantities are defined as:

$$\tau_{ij} = \overline{\rho}\,(\widetilde{u_i u_j} - \widetilde{u}_i\widetilde{u}_j) \tag{9}$$

$$Q_j = \overline{\rho}\left(\widetilde{u_j T} - \widetilde{u}_j\widetilde{T}\right) \tag{10}$$

$$\Pi_{dil} = \overline{pS_{kk}} - \overline{p}\widetilde{S}_{kk} \tag{11}$$

$$\varepsilon_v = \overline{\sigma_{ji}S_{ij}} - \widetilde{\sigma}_{ji}\widetilde{S}_{ij} \tag{12}$$

$$\mathcal{J}_j = \overline{\rho}\,(\widetilde{u_j u_k u_k} - \widetilde{u}_j\widetilde{u_k u_k}) \tag{13}$$

$$\mathcal{D}_j = \overline{\sigma_{ji}u_i} - \widetilde{\sigma}_{ji}\widetilde{u}_j. \tag{14}$$

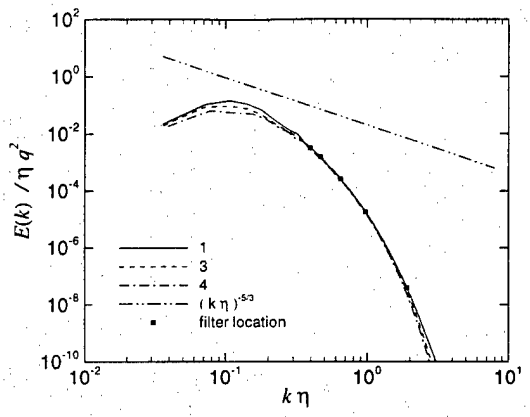

Figure 1. Energy spectra at $t/\tau_t = 1, 3$ and 4. The squares correspond to the filter-widths used in the *a priori* tests.

The equation of state has been used to express pressure-gradient and pressure-diffusion correlations in terms of Q_j and Π_{dil}. It is also assumed here that

$$\overline{\mu(T)S_{ij}} \simeq \mu(\widetilde{T})\widetilde{S}_{ij}, \tag{15}$$

and an equivalent equality involving the thermal conductivity applies. Vreman *et al.* (1995b) performed *a priori* tests using DNS data obtained from the calculation of a mixing layer at Mach numbers in the range 0.2–0.6, and concluded that neglecting the nonlinearities of the diffusion terms in the momentum and energy equations is acceptable.

2.2 A priori tests

One method to evaluate the performance of models for LES or RANS calculations is the *a priori* test, in which the velocity fields obtained from a direct simulation are filtered to yield the exact SGS terms, and the filtered quantities are used in a modeling *ansatz* to evaluate the accuracy of the parameterization. The database used in this study was obtained from the calculation of homogeneous isotropic turbulence decay.

The Navier-Stokes equations were integrated in time using a fourth-order order Runge-Kutta method. The spatial derivatives were computed using an eighth-order accurate central finite-difference scheme. The simulations were performed on grids with 256^3 points, so that a large range of scales is found in the energy spectrum. The computational domain is a periodic box with length 2π in each dimension. The fluctuating fields were initialized as in Martín and Candler (1996) and the DNS results were validated by comparison with the Martín and Candler (1996) simulations.

The calculation was performed at a Reynolds number $Re_\lambda = u'\lambda/\nu = 35$, where λ is the Taylor micro-scale and u' is the turbulence intensity, and at a turbulent Mach number $M_t = q/a = 0.52$, where $q^2 = u_i u_i$ and a is the speed of sound. Since the dilatational field is initially zero, the flow is allowed to evolve for one dimensionless time unit, $\tau_t = \lambda/u'$.

The subgrid scale quantities were then evaluated. The DNS fields were filtered using a top-hat filter

$$\overline{f}_i = \frac{1}{2n}\left(f_{i-\frac{n}{2}} + 2\Sigma_{i-\frac{n}{2}+1}^{i+\frac{n}{2}-1} f_i + f_{i+\frac{n}{2}}\right) \tag{16}$$

with varying filter widths $\overline{\Delta} = n\Delta$, where Δ is the grid size and $n = 2, 4, 6, 8$ and 10. Figure 1 shows the energy spectrum including the location of the filter cutoffs. All the filter-widths tested lie in the decaying region of the spectrum. Most of the results will be shown for a filter-width $\overline{\Delta} = 8\Delta$, at the edge of the inertial range of the spectrum. With this filter width approximately 11% of the energy resides in the subgrid-scales, a value representative of actual LES. Two quantities are used to evaluate the accuracy of a model: the correlation coefficient of the modeled term with the exact one, defined as

$$C(f) = \frac{\langle f_{\text{model}} f_{\text{DNS}} \rangle}{rms(f_{\text{model}})\, rms(f_{\text{DNS}})}, \tag{17}$$

and the L_2-norm of the modeled and exact terms.

3 Models for the momentum equation

The modeling of the SGS stresses has received comparatively more attention than any of the other unclosed terms in compressible flows. Yoshizawa (1986) proposed an eddy-viscosity model for weakly compressible turbulent flows using a multi-scale direct-interaction approximation method. The anisotropic part of the SGS stresses is parameterized using the Smagorinsky (1963) model, while the SGS energy τ_{kk} is modeled separately:

$$\tau_{ij} - \frac{\delta_{ij}}{3}\tau_{kk} = -C_s^2 2\overline{\Delta}^2 \overline{\rho}\,|\widetilde{S}|\left(\widetilde{S}_{ij} - \frac{\delta_{ij}}{3}\widetilde{S}_{kk}\right) = C_s^2 \alpha_{ij} \tag{18}$$

$$\tau_{kk} = C_I 2\overline{\rho}\,\overline{\Delta}^2 |\widetilde{S}|^2 = C_I \alpha \tag{19}$$

with $C_s = 0.16$ and $C_I = 0.09$.

Speziale *et al.* (1988) proposed the addition of a scale-similar part to the eddy-viscosity model of Yoshizawa. Scale-similar models are based on the assumption that the most active subgrid scales are those closer to the cutoff wavenumber, and that the scales with which they interact most are those right above the cutoff (Bardina *et al.*, 1980). The mixed model proposed by

Speziale *et al.* (1988), and used by Erlebacher *et al.* (1992) and Zang *et al.* (1992) was given by

$$\tau_{ij} - \frac{\delta_{ij}}{3}\tau_{kk} = C_s\alpha_{ij} + A_{ij} - \frac{\delta_{ij}}{3}A_{kk} \tag{20}$$

$$\tau_{kk} = C_I\alpha + A_{kk}, \tag{21}$$

where $A_{ij} = \overline{\rho}\,(\widetilde{\widetilde{u_i}\widetilde{u}_j} - \widetilde{\widetilde{u}}_i\widetilde{\widetilde{u}}_j)$. Erlebacher *et al.* (1992) tested the constant coefficient model *a priori* and by comparing DNS and LES results of compressible isotropic turbulence and found good agreement in the dilatational statistics of the flow, as well as high correlation between the exact and the modeled stresses. Zang *et al.* (1992) compared the DNS and LES results of isotropic turbulence with various initial ratios of compressible to total kinetic energy. They obtained good agreement for the evolution of quantities such as compressible kinetic energy and fluctuations of the thermodynamic variables.

Moin *et al.*(1991) proposed a modification of the eddy-viscosity model (18–19) in which the two model coefficients were determined dynamically, rather than input *a priori*, using the identity (Germano 1992) $\mathcal{L}_{ij} = T_{ij} - \widehat{\tau_{ij}}$, which relates the "resolved turbulent stresses",

$$\mathcal{L}_{ij} = \left(\widehat{\overline{\rho u_i}\,\overline{\rho u_j}/\overline{\rho}}\right) - \widehat{\overline{\rho u_i}}\,\widehat{\overline{\rho u_j}}/\widehat{\overline{\rho}}\,, \tag{22}$$

the subgrid-scale stresses τ_{ij} and the subtest stresses $T_{ij} = \widehat{\overline{\rho}}\,\widehat{\widetilde{u_i}\widetilde{u}_j} - \widehat{\overline{\rho}}\,\breve{\tilde{u}}_i\breve{\tilde{u}}_j$, where $\breve{\tilde{f}} = \widehat{\overline{\rho f}}/\widehat{\overline{\rho}}$, and the hat represents the application of the test filter $\widehat{G}$, of characteristic width $\widehat{\Delta} = 2\overline{\Delta}$. Moin *et al.* (1991) determined the model coefficients by substituting the models (18–19) into (22) and contracting with $\widetilde{S}_{ij}$; in this work the contraction proposed by Lilly (1992) to minimize the error in a least-squares sense will be used instead. Accordingly, the two model coefficients for the Dynamic Eddy-Viscosity model (denoted hereafter by the acronym DEV) will be given by

$$C = C_s^2 = \frac{\langle \mathcal{L}_{ij}M_{ij}\rangle}{\langle M_{kl}M_{kl}\rangle} - \frac{1}{3}\frac{\langle \mathcal{L}_{mm}M_{nn}\rangle}{\langle M_{kl}M_{kl}\rangle}, \qquad C_I = \frac{\langle \mathcal{L}_{kk}\rangle}{\langle \beta - \widehat{\alpha}\rangle}, \tag{23}$$

where $\beta_{ij} = -2\widehat{\Delta}^2\widehat{\overline{\rho}}\,|\breve{\tilde{S}}|(\breve{\tilde{S}}_{ij} - \delta_{ij}\breve{\tilde{S}}_{kk}/3)$, $M_{ij} = \beta_{ij} - \widehat{\alpha_{ij}}$, $\beta = 2\widehat{\Delta}^2\widehat{\overline{\rho}}\,|\breve{\tilde{S}}|^2$, and the brackets $\langle\cdot\rangle$ denote averaging over the computational volume. Dynamic model adjustment can be also applied to the mixed model (20–21), to yield the Dynamic Mixed model (DMM)

$$C = \frac{\langle \mathcal{L}_{ij}M_{ij}\rangle - \langle N_{ij}M_{ij}\rangle}{\langle M_{lk}M_{lk}\rangle} - \frac{1}{3}\frac{\langle \mathcal{L}_{mm}M_{nn}\rangle + \langle N_{mm}M_{nn}\rangle}{\langle M_{lk}M_{lk}\rangle} \tag{24}$$

$$C_I = \frac{\langle \mathcal{L}_{kk} - N_{kk}\rangle}{\langle \beta - \widehat{\alpha}\rangle}, \tag{25}$$

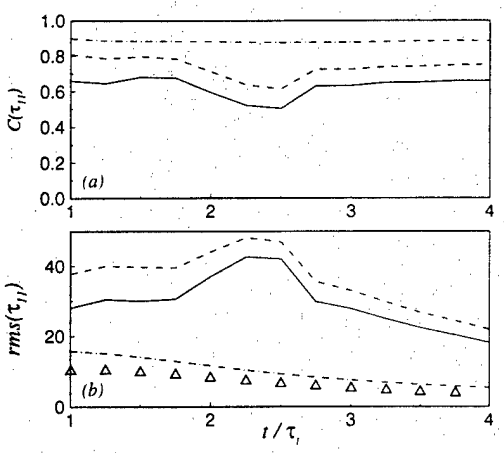

Figure 2. *A priori* comparison of the normal SGS stresses τ_{11}. —— DEV; - - - DMM; —·— DMM-1; △ DNS. (a) Correlation coefficient; (b) *rms* fluctuations.

with $B_{ij} = \widehat{\overline{\rho}}\,(\widehat{\breve{\tilde{u}}_i\breve{\tilde{u}}_j} - \widehat{\breve{\tilde{u}}_i}\,\widehat{\breve{\tilde{u}}_j})$, and $N_{ij} = B_{ij} - \widehat{A_{ij}}$. One advantage of mixed models is that they allow one to model the trace of the SGS stresses without requiring a separate term of the form (19). A one-coefficient dynamic mixed model (DMM-1) would be of the form

$$\tau_{ij} = C\alpha_{ij} + A_{ij}, \tag{26}$$

with

$$C = \frac{\langle \mathcal{L}_{ij}M_{ij}\rangle - \langle N_{ij}M_{ij}\rangle}{\langle M_{lk}M_{lk}\rangle}. \tag{27}$$

Figures 2 and 3 compare the diagonal and off-diagonal components of the SGS stress tensor predicted by the various models. Consistent with the results of previous investigators eddy-viscosity models are not to be able to predict the *rms* of the SGS stresses very accurately. All models have high correlation with the DNS data, although, for the DEV model, that is due to the trace of τ_{kk}. The eddy-viscosity prediction of the off-diagonal terms (Fig. 3) has, in fact, a much lower correlation coefficient. In general, the one-coefficient mixed model (26–27) appears to be the most accurate among those tested. Its correlation with the exact SGS stresses is always greater than 0.8, and the prediction of the *rms* is consistently more accurate than that of the eddy-viscosity model (and is also more accurate than that obtained with the two-coefficient mixed model, in which the SGS energy is modeled separately).

The coefficient C_s remained nearly constant at a value of 0.15 throughout the calculation, consistent with the theoretical arguments (Yoshizawa 1986). The coefficient of the SGS energy, C_I, on the other hand, has a value three times higher than

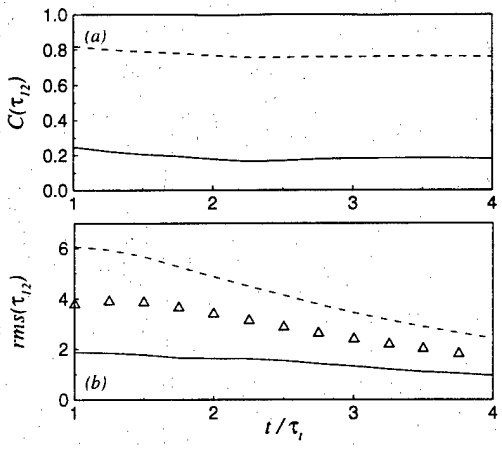

Figure 3. *A priori* comparison of the off-diagonal SGS stresses τ_{12}. ——— DEV; – – – DMM and DMM-1; △ DNS. (a) Correlation coefficient; (b) *rms* fluctuations.

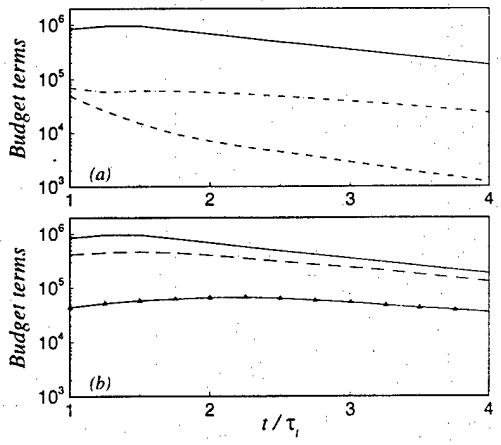

Figure 4. Comparison of unclosed terms in the energy equations. (a) Terms in the internal energy or enthalpy equations; (b) total energy equation. ——— Divergence of the SGS heat flux, $\partial Q_j/\partial x_j$; —·— SGS viscous dissipation ε_v; – – – pressure dilatation Π_{dil}; ——— SGS turbulent diffusion $\partial \mathcal{J}_j/\partial x_j$; —△— SGS viscous diffusion $\partial \mathcal{D}_j/\partial x_j$.

predicted by the theory, consistent with the results of Moin *et al.* (1991).

4 Models for the energy equations

A comparison of the magnitude of the unclosed terms in the three forms of the energy equation (5), (6) and (7) is shown in Fig. 4. Unlike in the mixing layer studied by Vreman *et al.* (1995b), in this flow the pressure dilatation Π_{dil} is negligible, and the viscous dissipation ε_v is less than one-tenth of the divergence of the SGS heat flux. Thus, the only term that requires modeling in the internal energy or enthalpy equations is Q_j. In the total energy equation, on the other hand, the SGS turbulent diffusion $\partial \mathcal{J}_j/\partial x_j$ is significant. In the following, several models for the more significant terms will be examined.

The most important term to be closed (Fig. 4) is the divergence of the SGS heat flux (10). The simplest approach is to use an eddy-diffusivity model of the form:

$$Q_j = -\frac{\overline{\rho}\nu_T}{Pr_T}\frac{\partial \widetilde{T}}{\partial x_j} = -C\frac{\overline{\Delta}^2\overline{\rho}|\widetilde{S}|}{Pr_T}\frac{\partial \widetilde{T}}{\partial x_j}, \tag{28}$$

where C is the eddy-viscosity coefficient in (23). The turbulent Prandtl number Pr_T can be fixed, or adjusted dynamically according to $Pr_T = C\langle T_k T_k\rangle/\langle \mathcal{K}_j T_j\rangle$, where

$$\mathcal{K}_j = \left(\widehat{\overline{\rho u_j}\overline{\rho T}}/\overline{\rho}\right) - \widehat{\overline{\rho u_j}}\,\widehat{\overline{\rho T}}/\widehat{\overline{\rho}}\,, \tag{29}$$

$$T_j = -\widehat{\Delta}^2\widehat{\overline{\rho}}\,\widehat{|\widetilde{S}|}\frac{\partial \widehat{\widetilde{T}}}{\partial x_j} + \widehat{\overline{\Delta}^2\overline{\rho}|\widetilde{S}|}\frac{\partial \widetilde{T}}{\partial x_j}. \tag{30}$$

A mixed model of the form

$$Q_j = -C\frac{\overline{\Delta}^2\overline{\rho}|\widetilde{S}|}{Pr_T}\frac{\partial \widetilde{T}}{\partial x_j} + \left(\widetilde{\widetilde{u}_j\widetilde{T}} - \widetilde{\widetilde{u}}_j\widetilde{\widetilde{T}}\right) \tag{31}$$

was proposed by Speziale *et al.* (1988). The model coefficient C is given by (24); Pr_T can again be assigned *a priori* or adjusted dynamically according to

$$Pr_T = C\frac{\langle T_k T_k\rangle}{\langle \mathcal{K}_j\mathcal{K}_j\rangle - \langle V_j T_j\rangle}, \tag{32}$$

with

$$V_j = \widehat{\overline{\rho}}\left(\widehat{\widetilde{\widetilde{u}}_j\widetilde{\widetilde{T}}} - \widehat{\widetilde{\widetilde{u}}}_j\widehat{\widetilde{\widetilde{T}}}\right) - \overline{\rho}\left(\widehat{\widetilde{u}_j\widetilde{T}} - \widehat{\widetilde{u}}_j\widehat{\widetilde{T}}\right). \tag{33}$$

In Figure 5 the models described above are compared. The eddy-diffusivity models have poor correlation with the DNS data, as is the case with these types of model. The constant-Pr_T case (the value used was 0.7, following Zang *et al.* 1992) gives a very low value of the *rms* of the modeled Q_j. A lower value, $Pr_T = 0.4$, as used by Speziale *et al.* (1988) would, however, give *rms* fluctuations nearly identical to those predicted using the dynamic procedure. The mixed model gives the best correlation with the data (again around 0.8), but over-predicts the *rms*; at early times the mixed model gives results in better agreement with the data than the eddy-diffusivity one, but for $t/\tau_t > 3$ the latter gives

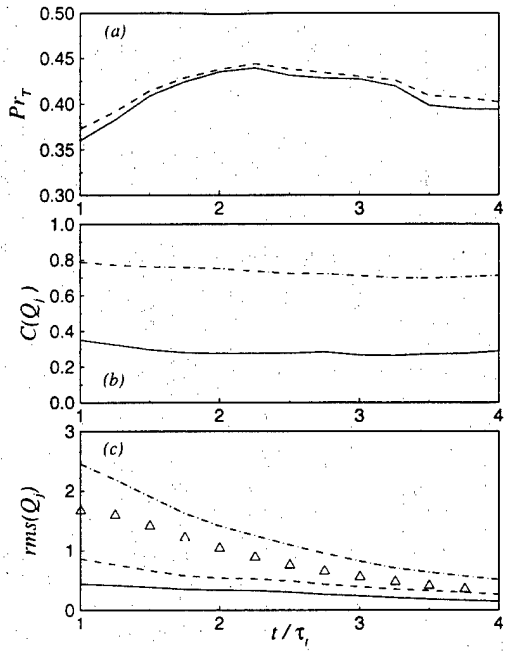

Figure 5. Coefficient, correlation and *rms* of the model for the SGS heat flux Q_j. (a) Turbulent Prandtl number, Pr_T; (b) correlation coefficient; (c) *rms*. ——— Eddy-diffusivity model, fixed Prandtl number; – – – eddy-diffusivity model, variable Prandtl number; —·— mixed model; △ DNS.

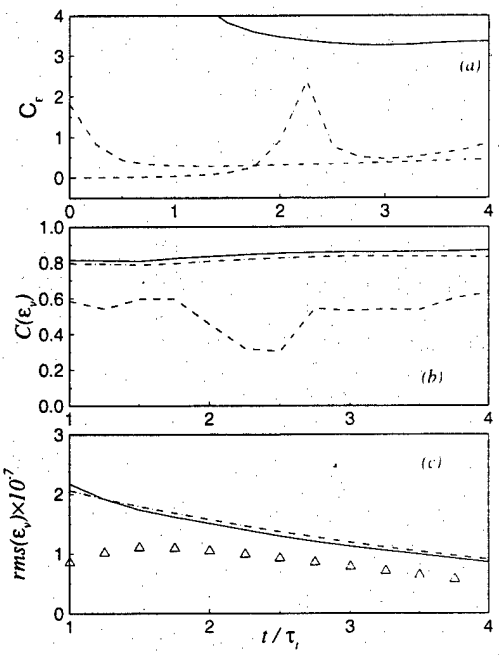

Figure 6. Coefficient, correlation and *rms* of the model for the viscous dissipation ε_v. (a) Model coefficient; (b) correlation coefficient; (c) *rms*. ——— Scale similar (34); – – – Dynamic (35); —·— Dynamic (36); △ DNS.

more accurate results. A limitation of this study is the fact that the filter width is already in the decaying region of the spectrum, a situation that has been shown to degrade the accuracy of the dynamic procedure (Lund and Meneveau 1997).

The other term that can be significant in the enthalpy or internal energy equations is the viscous dissipation ε_v. Vreman *et al.* (1995b) proposed three models for this term:

$$\varepsilon_v^{(1)} = C_{\varepsilon 1}\left(\widetilde{\widetilde{\sigma}_{ji}\widetilde{S}_{ij}} - \widetilde{\widetilde{\sigma}}_{ij}\widetilde{\widetilde{S}}_{ij}\right); \tag{34}$$

$$\varepsilon_v^{(2)} = C_{\varepsilon 2}\overline{\rho}\,\widetilde{q}^3/\overline{\Delta}, \qquad \widetilde{q}^2 \sim \overline{\Delta}^2|\widetilde{S}|^2; \tag{35}$$

$$\varepsilon_v^{(3)} = C_{\varepsilon 3}\overline{\rho}\,\widetilde{q}^3\overline{\Delta}, \qquad \widetilde{q}^2 \sim \widetilde{\widetilde{u}_k\widetilde{u}_k} - \widetilde{\widetilde{u}}_k\widetilde{\widetilde{u}}_k. \tag{36}$$

The first is a scale-similar model; the second and third use dimensional analysis to represent the SGS dissipation as the ratio between the cube of the SGS velocity scale, $\widetilde{q}$, and the length scale, and assign the velocity scale using either the Yoshizawa (1986) model (19) or the scale-similar model. For consistency, each of the last two models should be coupled with the corresponding model for τ_{kk}. Based on their DNS data, Vreman *et al.* (1995b) fixed the values of the coefficients that give the correct magnitude for this term and obtained: $C_{\varepsilon 1} = 8$, $C_{\varepsilon 2} = 1.6$ and $C_{\varepsilon 3} = 0.6$. Alternatively, the dynamic procedure can be used to give

$$\left\langle \widehat{\widetilde{\sigma}_{ji}\widetilde{S}_{ij}} - \widehat{\overline{\rho}\overline{\sigma}_{ij}}\,\widehat{\overline{\rho}\widetilde{S}_{ij}}/\widehat{\overline{\rho}}^{\,2} \right\rangle = \left\langle E_v^{(n)} - \widehat{\varepsilon_v^{(n)}} \right\rangle. \tag{37}$$

where

$$E_v^{(1)} = C_{\varepsilon 1}\left(\widetilde{\overset{\sim}{\sigma}_{ji}\tilde{S}_{ij}} - \overset{\sim}{\sigma}_{ij}\tilde{S}_{ij}\right); \tag{38}$$

$$E_v^{(2)} = C_{\varepsilon 2}\widehat{\overline{\rho}}\,\tilde{q}^3/\widehat{\Delta}, \qquad \tilde{q}^2 \sim \widehat{\Delta}^2|\tilde{S}|^2; \tag{39}$$

$$E_v^{(3)} = C_{\varepsilon 3}\widehat{\overline{\rho}}\,\tilde{q}^3/\widehat{\Delta}, \qquad \tilde{q}^2 \sim \widetilde{\tilde{u}_i\tilde{u}_j} - \tilde{u}_i\tilde{u}_j. \tag{40}$$

Model coefficients obtained from the dynamic procedure in this form (in which there is no contraction) can become ill-conditioned, since the two terms in the denominator may be approximately equal, giving spuriously high values of the denominator. This behavior was observed in model (34), in which acceptable results were obtained only if $C_{\varepsilon 1}$ was constrained to be positive, and model (35). The model given by (36), on the other hand, was well behaved.

Figure 6 compares the predictions of the three models. The values of the coefficients obtained from the present *a priori* test

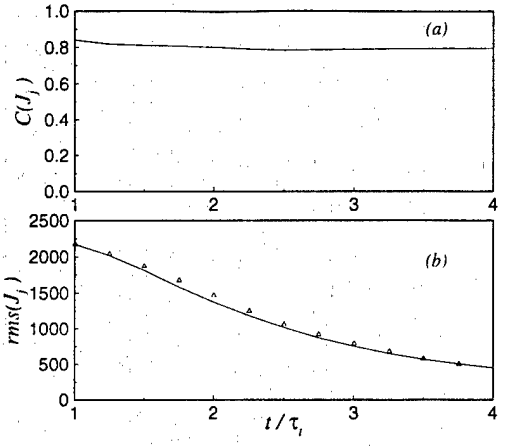

Figure 7. Correlation and *rms* of the model for the turbulent diffusion $\mathcal{J}_j$. (a) correlation coefficient; (b) *rms*. ——— Knight *et al.* (1998) model; △ DNS.

are lower than those obtained in the mixing layer by Vreman *et al.* (1995b). The pure scale-similar model (34) and the model (36), which also uses scale similarity to supply the velocity scale, give the best correlation and nearly correct *rms* amplitudes. The *rms* predicted by the model (35) is two orders of magnitude larger than the others, and cannot be seen in the plot. In this flow the coefficients obtained from the mixing layer data would yield high values of the modeled *rms*, indicating some lack of universality for the modeling of this term.

The two terms in the total energy equation that require modeling are the SGS turbulent diffusion $\partial \mathcal{J}_j/\partial x_j$ and the SGS viscous diffusion $\partial \mathcal{D}_j/\partial x_j$. The only calculation that attempted to model the former was that by Knight *et al.* (1998). They argued that $\widetilde{u}_i \simeq \widetilde{\widetilde{u}}_i$ and proposed a model of the form

$$\mathcal{J}_j \simeq \widetilde{u}_k \tau_{jk}. \tag{41}$$

This model is compared in Fig. 7 with the DNS data; τ_{jk} was obtained from the DMM-1 model (41). The model has a high correlation with the data (of order 0.8), and the *rms* also matches the data well. It should be noticed, however, that the model is built upon the prediction of the SGS stresses by DMM-1, which over-predicts the *rms* of the normal stresses by 30%, that of the off-diagonal ones by about 50%. It appears that the modeling assumption by itself might underestimate the diffusion, an error that is compensated by one of opposite sign in the SGS stress model. The high correlation, however, indicates that addition of a model coefficient, perhaps adjusted dynamically, may be beneficial.

The SGS viscous diffusion $\partial \mathcal{D}_j/\partial x_j$ is the smallest of the terms in the total energy equation. It is 5% of the divergence of Q_j at $t/\tau_t = 1$, but increases to about 10% at the final time. No

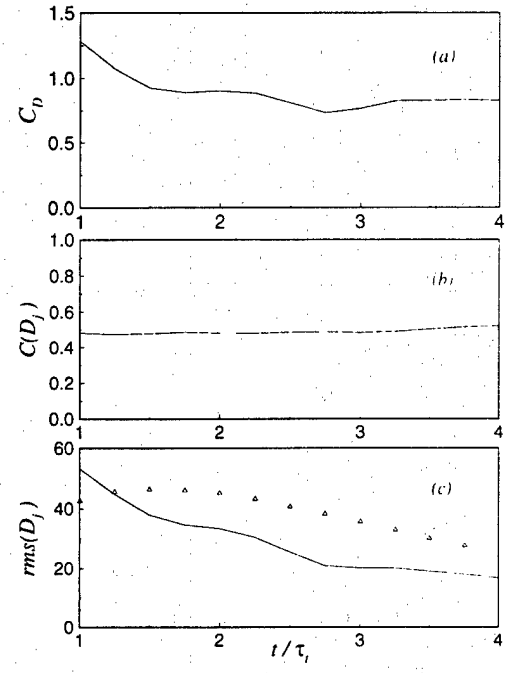

Figure 8. Coefficient, correlation and *rms* of the model for the viscous diffusion $\mathcal{D}_j$. (a) Model coefficient; (b) correlation coefficient; (c) *rms*. ——— Scale-similar model; △ DNS.

model for this term has been proposed in the literature to date. One possibility is to parameterize it using a scale-similar model of the form

$$\mathcal{D}_j = C_D(\widetilde{\widetilde{\sigma}_{ij}\widetilde{u}_i} - \widetilde{\widetilde{\sigma}}_{ij}\widetilde{\widetilde{u}}_i), \tag{42}$$

in which the coefficient can be obtained from

$$C_D = \frac{\left\langle \left[\widehat{\frac{\overline{\rho}\sigma_{ij}\overline{\rho}u_i}{\overline{\rho}^2}} - \frac{\widehat{\overline{\rho}\sigma}_{ij}\widehat{\overline{\rho}u}_i}{\widehat{\overline{\rho}}^2} \right] \mathcal{R}_j \right\rangle}{\langle \mathcal{R}_k \mathcal{R}_k \rangle}, \tag{43}$$

where

$$\mathcal{R}_l = \left(\widehat{\widetilde{\sigma}_{lk}\widetilde{u}_k} - \widehat{\widetilde{\sigma}}_{lk}\widehat{\widetilde{u}}_k \right) - \left(\widehat{\widetilde{\sigma}_{lk}\widetilde{u}_k} - \widehat{\widetilde{\sigma}}_{lk}\widehat{\widetilde{u}}_k \right). \tag{44}$$

As can be seen from Fig. 8, however, this approach gives a fairly poor correlation, and fair agreement for the prediction of the *rms* intensities. This error may, however, be tolerable given the small contribution that this term gives to the energy budget.

5 Conclusions

Several mixed and eddy-viscosity models for the momentum and energy equations have been tested. The velocity, pressure, density and temperature fields obtained from the DNS of homogeneous isotropic turbulence at $Re_\lambda = 35$, $M_t = 0.52$ were filtered and the unclosed terms in the momentum, internal energy and total energy equations were computed.

In the momentum equation, mixed models were found to give better prediction, in terms of both correlation and *rms* amplitude, than the pure eddy-viscosity models. The dynamic adjustment of the model coefficient was beneficial, as already observed by Moin *et al.* (1991).

In the internal energy and enthalpy equations, in this flow, only the divergence of the SGS heat flux was significant; the SGS pressure dilatation Π_{dil} and viscous dissipation ε_v, which were significant in the mixing layer studied by Vreman *et al.* (1995b), were found to be negligible here. Once again, mixed dynamic models gave the most accurate results. In particular, the turbulent Prandtl number obtained dynamically was somewhat lower than the value of 0.7 often assigned *a priori*.

In the total energy equation two additional terms are present, one of which, the turbulent diffusion $\partial \mathcal{J}_j / \partial x_j$ is significant. The model proposed by Knight *et al.* (1998), which parameterizes the turbulent diffusion in terms of the SGS stresses, correlates well with the actual SGS stresses, and predicts the correct *rms* amplitude. A mixed model for the SGS turbulent diffusion has also been proposed and tested, although this term is much smaller than the others.

Although the preliminary results obtained in this investigation are promising, and indicate that it is possible to model the terms in the energy equations, and in particular in the total energy one, accurately, further work is required to extend these results to cases in which the pressure-dilatation is significant, as well as to inhomogeneous flows. *A posteriori* testing of the models in actual calculations is also necessary for a complete evaluation of the model performance.

Acknowledgments

The authors gratefully acknowledge the support from the Air Force Office of Scientific Research, under Grants No. AF/F49620-98-1-0035 (MPM and GVC) and AF/F49620-97-1-0244 (UP), monitored by Dr. L. Sakell. This work was also sponsored by the Army High Performance Computing Research Center under the auspices of the Department of the Army, Army Research Laboratory cooperative agreement number DAAH04-95-2-0003 / contract number DAAH04-95-C-0008, the content of which does not necessarily reflect the position or the policy of the government, and no official endorsement should be inferred. A portion of the computer time was provided by the University of Minnesota Supercomputing Institute.

REFERENCES

Bardina, J., Ferziger, J. H., and Reynolds, W. C. *AIAA Paper No. 80–1357* (1980).

El-Hady, N., Zang, T. A. , and Piomelli, U. *Phys. Fluids* **6**, 1299 (1994).

Erlebacher, G., Hussaini, M. Y., Speziale, C. G., and Zang, T. A. *J. Fluid Mech.* **238**, 155 (1992).

Favre, A. *J. de Mécanique* **4**, 361 (1965a).

Favre, A. *J. de Mécanique* **4**, 391 (1965b).

Germano, M. *J. Fluid Mech.* **238**, 325–336 (1992).

Knight, D., Zhou, G., Okong'o, N., and Shukla, V. *AIAA Paper 98-0535* (1998).

Leonard, A. *Adv. Geophys.* **18A**, 237 (1974).

Liu, S., Meneveau, C., and Katz, J. *J. Fluid Mech.* **275**, 83.

Lund, T. S., and Meneveau, C. *Phys. Fluids* **9**, 3982 (1997).

Martín, M. P., and Candler, G.V. *AIAA Paper 96-2060* (1996).

Moin, P., Squires, K. D., Cabot, W. H., and Lee, S. *Phys. Fluids A* **3**, 2746 (1991).

Normand, X. and Lesieur, M. *Theoret. Comput. Fluid Dyn.* **3**, 231 (1992).

Speziale, C. G., Erlebacher, G., Zang, T. A., and Hussaini, M. Y. *Phys. Fluids A* **31**, 940 (1988).

Smagorinsky, J. *Monthly Weather Review* **91**, 99 (1963).

Vreman, B., Geurts, B., and Kuerten, H. *J. Eng. Math.* **29**, 299 (1995a).

Vreman, B., Geurts, B., and Kuerten, H. *Applied Sci. Res.* **54**, 191 (1995b).

Yoshizawa, A. *Phys. Fluids A* **29**, 2152 (1986).

Zang, T. A., Dahlburg, R. B., and Dahlburg, J. P. *Phys. Fluids A* **4**, 127 (1992).

Zang, Y., Street, R. L., and Koseff, J. *Phys. Fluids A* **5**, 3186 (1993).

Subgrid-Scale Models for Compressible Large-Eddy Simulations

M. Pino Martín[1]
Department of Aerospace Engineering and Mechanics
University of Minnesota
110 Union St. SE, Minneapolis, MN 55455
pino@aem.umn.edu / Fax: 612-626-1596

Ugo Piomelli
Department of Mechanical Engineering
University of Maryland
College Park, MD 20742
ugo@eng.umd.edu / Fax: 301-314-9477

Graham V. Candler
Department of Aerospace Engineering and Mechanics
University of Minnesota
110 Union St. SE, Minneapolis, MN 55455
candler@aem.umn.edu / Fax: 612-626-1558

Submitted to
Theoretical and Computational Fluid Dynamics
March 15, 1999

[1]Corresponding author.

Abstract

An *a priori* study of subgrid-scale models for the unclosed terms in the energy equation is carried out using the flow field obtained from the direct simulation of homogeneous isotropic turbulence. Scale-similar models involve multiple filtering operations to identify the smallest resolved scales that have been shown to be the most active in the interaction with the unresolved subgrid scales (SGS). In the present study these models are found to give more accurate prediction of the SGS stresses and heat fluxes than eddy-viscosity and eddy-diffusivity models, as well as improve prediction of the SGS turbulent diffusion, SGS viscous dissipation, and SGS viscous diffusion.

2 Governing equations

To obtain the equations governing the motion of the resolved eddies, we must separate the large from the small scales. LES is based on the definition of a filtering operation: a resolved variable, denoted by an overbar, is defined as (Leonard, 1974)

$$\overline{f}(\mathbf{x}) = \int_D f(\mathbf{x}')G(\mathbf{x},\mathbf{x}';\overline{\Delta})d\mathbf{x}'. \tag{1}$$

where D is the entire domain and G is the filter function, and $\overline{\Delta}$ is the filter-width associated with the wavelength of the smallest scale retained by the filtering operation. Thus, the filter function determines the size and structure of the small scales

In compressible flows, it is convenient to use Favre-filtering (Favre, 1965a,b) to avoid the introduction of subgrid-scale terms in the equation of conservation of mass. A Favre-filtered variable is defined as $\widetilde{f} = \overline{\rho f}/\overline{\rho}$. In addition to the mass and momentum equations, one can choose solving an equation for the internal energy, enthalpy or total energy. Applying the Favre-filtering operation, we obtain the resolved transport equations

$$\frac{\partial \overline{\rho}}{\partial t} + \frac{\partial}{\partial x_j}\left(\overline{\rho}\,\widetilde{u}_j\right) = 0. \tag{2}$$

$$\frac{\partial \overline{\rho}\,\widetilde{u}_i}{\partial t} + \frac{\partial}{\partial x_j}\left(\overline{\rho}\,\widetilde{u}_i\widetilde{u}_j + \overline{p}\delta_{ij} - \widetilde{\sigma}_{ji}\right) = \frac{\partial \tau_{ji}}{\partial x_j}, \tag{3}$$

$$\frac{\partial(\overline{\rho}\,\widetilde{e})}{\partial t} + \frac{\partial}{\partial x_j}\left(\overline{\rho}\,\widetilde{u}_j\widetilde{e}\right) + \frac{\partial \widetilde{q}_j}{\partial x_j} + \overline{p}\widetilde{S}_{kk} - \widetilde{\sigma}_{ji}\widetilde{S}_{ij} = C_v\frac{\partial Q_j}{\partial x_j} - \Pi_{dil} + \epsilon_v, \tag{4}$$

$$\frac{\partial(\overline{\rho}\,\widetilde{h})}{\partial t} + \frac{\partial}{\partial x_j}\left(\overline{\rho}\,\widetilde{u}_j\widetilde{h}\right) + \frac{\partial \widetilde{q}_j}{\partial x_j} - \frac{\partial \overline{p}}{\partial t} - \widetilde{u}_j\frac{\partial \overline{p}}{\partial x_j} - \widetilde{\sigma}_{ji}\widetilde{S}_{ij} = C_v\frac{\partial Q_j}{\partial x_j} - \Pi_{dil} + \epsilon_v, \tag{5}$$

$$\frac{\partial}{\partial t}(\overline{\rho}\,\widetilde{E}) + \frac{\partial}{\partial x_j}\left[(\overline{\rho}\,\widetilde{E} + \overline{p})\widetilde{u}_j + \widetilde{q}_j - \widetilde{\sigma}_{ji}\widetilde{u}_j\right] = \frac{\partial}{\partial x_j}\left(\gamma C_v Q_j + \frac{1}{2}\mathcal{J}_j - \mathcal{D}_j\right). \tag{6}$$

Here ρ is the density, u_j is the velocity in the x_j direction, p the pressure, $\epsilon = c_vT$ is the internal energy per unit mass, T the temperature, $h = \epsilon + p/\rho$ is the enthalpy per unit mass, $E = \epsilon + u_iu_i/2$ is the total energy per unit mass, and the diffusive fluxes are given by

$$\widetilde{\sigma}_{ij} = 2\widetilde{\mu}\widetilde{S}_{ij} - \frac{2}{3}\widetilde{\mu}\delta_{ij}\widetilde{S}_{kk}, \qquad \widetilde{q}_j = -\widetilde{k}\frac{\partial \widetilde{T}}{\partial x_j}, \tag{7}$$

where $S_{ij} = (\partial u_i/\partial x_i + \partial u_j/\partial x_i)$ is the strain rate tensor, and $\widetilde{\mu}$ and $\widetilde{k}$ are the viscosity and thermal conductivity corresponding to the filtered temperature $\widetilde{T}$.

The effect of the subgrid scales appears on the right hand side of the governing equations through the SGS stresses τ_{ij}; SGS heat flux Q_j; SGS pressure-dilatation Π_{dil}; SGS viscous dissipation ϵ_v; SGS turbulent diffusion $\partial\mathcal{J}_j/\partial x_j$; and SGS viscous diffusion $\partial\mathcal{D}_j/\partial x_j$. These quantities are defined as:

$$\tau_{ij} = \overline{\rho}\left(\widetilde{u_iu_j} - \widetilde{u}_i\widetilde{u}_j\right) \tag{8}$$

$$Q_j = \overline{\rho}\left(\widetilde{u_jT} - \widetilde{u}_j\widetilde{T}\right) \tag{9}$$

$$\Pi_{dil} = \overline{pS_{kk}} - \overline{p}\widetilde{S}_{kk} \tag{10}$$

$$\epsilon_v = \overline{\sigma_{ji}S_{ij}} - \widetilde{\sigma}_{ji}\widetilde{S}_{ij} \tag{11}$$

$$\mathcal{J}_j = \overline{\rho}\left(\widetilde{u_j\widetilde{u_ku_k}} - \widetilde{u}_j\widetilde{u_ku_k}\right) \tag{12}$$

$$\mathcal{D}_j = \overline{\sigma_{ji}u_i} - \widetilde{\sigma}_{ji}\widetilde{u}_i. \tag{13}$$

The equation of state has been used to express pressure-gradient and pressure-diffusion correlations in terms of Q_j and Π_{dil}. It is also assumed that $\overline{\mu(T)S_{ij}} \simeq \mu(\widetilde{T})\widetilde{S}_{ij}$, and that an equivalent equality involving the thermal conductivity applies. Vreman *et al.* (1995b) performed *a priori* tests using DNS data obtained from the calculation of a mixing layer at Mach numbers in the range 0.2 0.6, and concluded that neglecting the nonlinearities of the diffusion terms in the momentum and energy equations is acceptable.

3 *A priori* test

One method to evaluate the performance of models for LES or RANS calculations is the *a priori* test, in which the velocity fields obtained from a direct simulation are filtered to

τ_{kk} is modeled separately:

$$\tau_{ij} - \frac{\delta_{ij}}{3}\tau_{kk} = -C_s^2 2\overline{\Delta}^2 \overline{\rho}\,|\tilde{S}|\left(\tilde{S}_{ij} - \frac{\delta_{ij}}{3}\tilde{S}_{kk}\right) = C_s^2 \alpha_{ij}; \qquad \tau_{kk} = C_I 2\overline{\rho}\,\overline{\Delta}^2 |\tilde{S}|^2 = C_I \alpha \quad (16)$$

with $C_s = 0.16$ and $C_I = 0.09$.

Moin *et al.* (1991) proposed a modification of the eddy-viscosity model (??) in which the two model coefficients were determined dynamically, rather than input *a priori*, using the Germano identity $\mathcal{L}_{ij} = T_{ij} - \widehat{\tau_{ij}}$ (Germano, 1992), which relates the subgrid-scale stresses τ_{ij} to the "resolved turbulent stresses" $\mathcal{L}_{ij} = \left(\widehat{\overline{\rho u_i}\,\overline{\rho u_j}/\overline{\rho}}\right) - \widehat{\overline{\rho u_i}}\,\widehat{\overline{\rho u_j}}/\widehat{\overline{\rho}}$, and the subtest stresses $T_{ij} = \widehat{\overline{\rho}}\,\widetilde{u_i}\widetilde{u_j} - \widehat{\overline{\rho}}\,\tilde{\tilde{u}}_i\tilde{\tilde{u}}_j$ (where $\tilde{\tilde{f}} = \widehat{\overline{\rho f}}/\widehat{\overline{\rho}}$, and the hat represents the application of the test filter $\widehat{G}$ of characteristic width $\widehat{\Delta} = 2\overline{\Delta}$) that appear if the filter $\widehat{G}$ is applied to (??). Moin *et al.* (1991) determined the model coefficients by substituting (??) into the Germano identity and contracting with $\tilde{S}_{ij}$. In the present paper the contraction proposed by Lilly (1992) to minimize the error in a least-squares sense will be used instead. Accordingly, the two model coefficients for the Dynamic Eddy-Viscosity model (DEV) will be given by

$$C = C_s^2 = \frac{\langle \mathcal{L}_{ij} M_{ij}\rangle}{\langle M_{kl} M_{kl}\rangle}; \qquad C_I = \frac{\langle \mathcal{L}_{kk}\rangle}{\langle \beta - \widehat{\alpha}\rangle}, \quad (17)$$

where $\beta_{ij} = -2\widehat{\Delta}^2\widehat{\overline{\rho}}\,|\tilde{\tilde{S}}|(\tilde{\tilde{S}}_{ij} - \delta_{ij}\tilde{\tilde{S}}_{kk}/3)$, $M_{ij} = \beta_{ij} - \widehat{\alpha_{ij}}$, $\beta = 2\widehat{\Delta}^2\widehat{\overline{\rho}}\,|\tilde{\tilde{S}}|^2$.

Scale-similar models are based on the assumption that the most active subgrid scales are those closer to the cutoff, and that the scales with which they interact are those right above the cutoff wavenumber (Bardina *et al.*, 1980). Thus, scale-similar models employ multiple operations to identify the smallest resolved scales and use the smallest "resolved" stresses to represent the SGS stresses. Although these models account for the local energy events, they underestimate the dissipation.

Speziale *et al.* (1988) proposed the addition of a scale-similar part to the eddy-viscosity model of Yoshizawa (1986) introducing the mixed model. In this way, the eddy-viscosity contribution provides the dissipation that is underestimated by purely scale-similar models.

This mixed model was also used by Erlebacher *et al.* (1992) and Zang *et al.* (1992), and is given by

$$\tau_{ij} - \frac{\delta_{ij}}{3}\tau_{kk} = C_s\alpha_{ij} + A_{ij} - \frac{\delta_{ij}}{3}A_{kk}; \qquad \tau_{kk} = C_I\alpha + A_{kk}, \quad (18)$$

where $A_{ij} = \overline{\rho}\,(\widetilde{u_i u_j} - \tilde{\tilde{u}}_i\tilde{\tilde{u}}_j)$.

Erlebacher *et al.* (1992) tested the constant coefficient model *a priori* and by comparing DNS and LES results of compressible isotropic turbulence and found good agreement in the dilatational statistics of the flow, as well as high correlation between the exact and the modeled stresses. Zang *et al.* (1992) compared the DNS and LES results of isotropic turbulence with various initial ratios of compressible to total kinetic energy. They obtained good agreement for the evolution of quantities such as compressible kinetic energy and fluctuations of the thermodynamic variables.

Dynamic model adjustment can be also applied to the mixed model (??), to yield the Dynamic Mixed Model (DMM)

$$C = \frac{\langle \mathcal{L}_{ij} M_{ij}\rangle - \langle N_{ij} M_{ij}\rangle}{\langle M_{lk} M_{lk}\rangle}; \qquad C_I = \frac{\langle \mathcal{L}_{kk} - N_{kk}\rangle}{\langle \beta - \widehat{\alpha}\rangle}, \quad (19)$$

with $B_{ij} = \widehat{\overline{\rho}}\,(\widetilde{\tilde{u}_i\tilde{u}_j} - \tilde{\tilde{u}}_i\tilde{\tilde{u}}_j)$, and $N_{ij} = B_{ij} - \widehat{A_{ij}}$.

An issue that requires some attention is the necessity to model separately the trace of the SGS stresses τ_{kk}. Yoshizawa (1986), Moin *et al.* (1991) and Speziale *et al.* (1988) proposed a separate model for this term. Erlebacher *et al.* (1992) conjectured that, for turbulent Mach numbers $M_t < 0.4$ this term is negligible; their DNS of isotropic turbulence confirm this conjecture. Zang *et al.* (1992) confirmed these results *a posteriori*: they ran calculations with $0 \le C_I \le 0.066$ (the latter value is 10 times higher than that predicted by the theory) and observed little difference in the results.

Comte and Lesieur (1998) proposed incorporating this term into a modified pressure $\mathcal{P}$. This leads to the presence of an additional term in the equation of state, which takes the

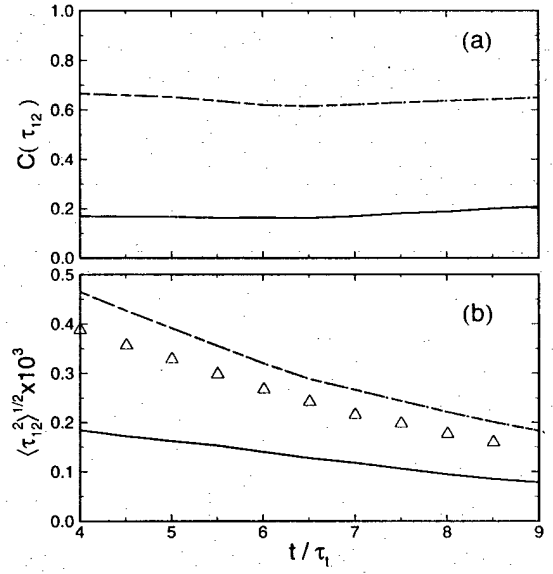

Figure 3: *A priori* comparison of the off-diagonal SGS stresses τ_{12}. (a) Correlation coefficient and (b) non-dimensional rms magnitude. —— Eddy-viscosity model DEV (?? ??); --- two-coefficient mixed model DMM (?? ??) and one-coefficient mixed model DMM-1 (?? ??); △ DNS.

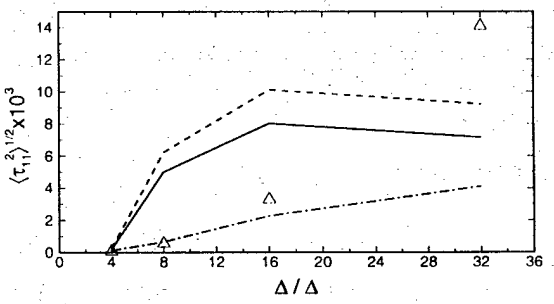

Figure 4: Non-dimensional rms magnitude of τ_{11} versus filter-width at $t/\tau_l = 6.5$. —— Eddy-viscosity model DEV (?? ??); --- two-coefficient mixed model DMM (?? ??); —·— one-coefficient mixed model DMM-1 (?? ??); △ DNS.

(near 0.2), while much improved results are obtained with the mixed models. Note that the correlation coefficient for DMM and DMM-1 overlap in the figure. Figure 3b shows the rms of τ_{12}. DEV under-predicts the rms magnitude of the exact term, while DMM and DMM-1 slightly over-predict it.

The coefficient C_s remained nearly constant at a value of 0.15 throughout the calculation, consistent with the theoretical arguments (Yoshizawa, 1986). The coefficient of the SGS energy, C_I, on the other hand, has a value three times higher than predicted by the theory, consistent with the results of Moin *et al.* (1991).

Figure 4 shows the rms magnitude of τ_{11} *vs.* the filter-width, at time $t/\tau_l = 6.5$. Consistent with the results shown above for $\overline{\Delta}/\Delta = 8$, the one-coefficient mixed model DMM gives the most accurate predictions. For very small filter widths ($\overline{\Delta}/\Delta = 2$), all the models are accurate, reflecting the capability of dynamic models to turn off the model contribution when the grid becomes sufficiently fine to resolve all the turbulent structures (models with constants assigned *a priori*, such as the Smagorinsky (1963) model, do not have this characteristic). For intermediate filter-widths, up to $\overline{\Delta}/\Delta = 16$, the best prediction is given by the

where

$$T_j = -\hat{\Delta}^2\hat{\overline{\rho}}\,|\hat{\tilde{S}}|\frac{\partial\hat{\tilde{T}}}{\partial x_j} + \overline{\Delta}^2\overline{\rho}\,\widehat{|\tilde{S}|\frac{\partial\tilde{T}}{\partial x_j}}, \qquad \mathcal{K}_j = \left(\widehat{\overline{\rho u_j}\,\overline{\rho T}}/\overline{\rho}\right) - \widehat{\overline{\rho u_j}}\,\widehat{\overline{\rho T}}/\hat{\overline{\rho}} \tag{25}$$

A mixed model of the form

$$Q_j = -C\frac{\overline{\Delta}^2\overline{\rho}|\tilde{S}|}{Pr_T}\frac{\partial\tilde{T}}{\partial x_j} + \overline{\rho}\left(\widetilde{\tilde{u}_j\tilde{T}} - \tilde{\tilde{u}}_j\tilde{\tilde{T}}\right) \tag{26}$$

was proposed by Speziale *et al.* (1988). The model coefficients C and Pr_T can again be assigned, or adjusted dynamically according to (??) and

$$Pr_T = C\frac{\langle T_k T_k\rangle}{\langle \mathcal{K}_j T_j\rangle - \langle V_j T_j\rangle}, \tag{27}$$

with

$$V_j = \hat{\overline{\rho}}\left(\widetilde{\tilde{u}_j\tilde{T}} - \tilde{\tilde{u}}_j\tilde{\tilde{T}}\right) - \overline{\rho}\left(\widehat{\tilde{u}_j\tilde{T}} - \tilde{\tilde{u}}_j\tilde{\tilde{T}}\right). \tag{28}$$

Figure 6a shows the correlation coefficient for the three models described above. Both eddy-viscosity models overlap on the plot giving a poor correlation factor, roughly 0.2, whereas the mixed model gives a correlation above 0.6. Both eddy viscosity models underpredict the rms of the exact Q_j, shown in Fig. 6b, while the mixed model is more accurate. The mixed model maintains accuracy for all filter-widths $\overline{\Delta}/\Delta \leq 16$ (Fig. 7).

5.2 SGS viscous dissipation

The other term in the enthalpy or internal energy equations that was found to be significant in the present flow is the viscous dissipation ϵ_v. In this section, the three models proposed by Vreman *et al.* (1995b) are tested:

$$\epsilon_v^{(1)} = C_{\epsilon 1}\left(\widetilde{\tilde{\sigma}_{ji}\tilde{S}_{ij}} - \tilde{\tilde{\sigma}}_{ij}\tilde{\tilde{S}}_{ij}\right); \tag{29}$$

$$\epsilon_v^{(2)} = C_{\epsilon 2}\overline{\rho}\,\widetilde{q}^3/\overline{\Delta}, \qquad \widetilde{q}^2 \sim \overline{\Delta}^2|\tilde{S}|^2; \tag{30}$$

$$\epsilon_v^{(3)} = C_{\epsilon 3}\overline{\rho}\,\widetilde{q}^3\overline{\Delta}, \qquad \widetilde{q}^2 \sim \widetilde{\tilde{u}_k\tilde{u}_k} - \tilde{\tilde{u}}_k\tilde{\tilde{u}}_k. \tag{31}$$

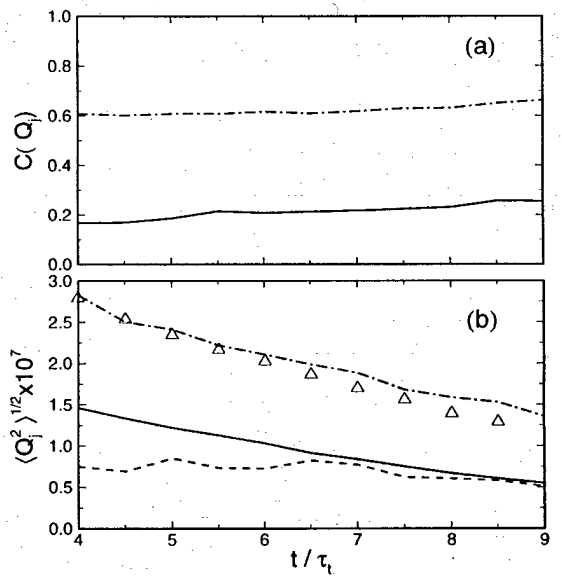

Figure 6: *A priori* comparison of the SGS heat flux Q_j. (a) Correlation coefficient and (b) non-dimensional rms magnitude. —— Eddy-diffusivity model (??), $Pr_T = 0.7$; --- eddy-diffusivity model (??), Prandtl number adjusted according to (??); —·— mixed model (?? ??); △ DNS.

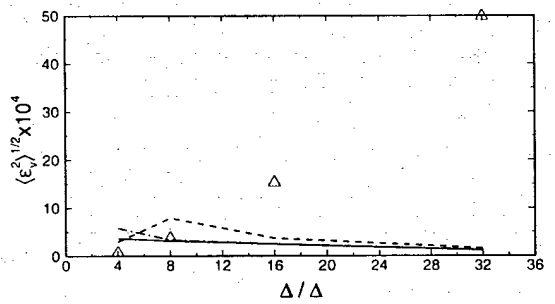

Figure 9: Non-dimensional rms magnitude of ϵ_v versus filter-width at $t/\tau_t = 6.5$. —— Scale similar model (33); --- Dynamic model (34); —·— Dynamic model (35); △ DNS.

Figure 8a shows the correlation coefficient for the three models. All models give a correlation coefficient above 0.7. The use of a velocity scale obtained from the scale-similar assumption, however, results in improved prediction of the rms magnitude; using $q \sim \overline{\Delta}|\tilde{S}|$ yields a significant over-prediction of the rms. The values of the coefficients obtained from the dynamic adjustment in this flow are significantly lower than those obtained in the mixing layer by Vreman *et al.* (1995b). For the particular filter-width shown, we obtained $C_{\epsilon 1} = 2.4$, and $C_{\epsilon 2} = 0.03$, while $C_{\epsilon 3}$ increased monotonically in time from 0.25 to 0.4. The fact that with these values the first and third models match the rms magnitude of the exact term indicates a lack of universality of these constants. Dynamic adjustment of the model coefficient appears to be beneficial for this term.

The modeling of the viscous dissipation is more sensitive than the other terms to the filter width. The prediction accuracy deteriorates with increasing filter-width, and in this case even for $\overline{\Delta}/\Delta = 16$ none of the models is particularly accurate (Fig. 9).

5.3 SGS turbulent diffusion

The SGS turbulent diffusion $\partial \mathcal{J}_j / \partial x_j$ appears in the total energy equation (??). Comte and Lesieur (1998) did not model this term explicitly, but added it to the SGS heat flux by using an eddy-diffusivity model to parameterize

$$\left(\widetilde{\rho E u_j} + \widetilde{p u_j}\right) - \left(\overline{\rho}\,\widetilde{E}\widetilde{u}_j + \overline{p}\widetilde{u}_j\right) \quad \gamma\overline{\rho}\left(\widetilde{u_j T} - \widetilde{u}_j\widetilde{T}\right) + \mathcal{J}_j \simeq -\frac{\nu_T}{Pr_T}\frac{\partial \widetilde{T}}{\partial x_j}; \tag{36}$$

with this model, however, the SGS turbulent diffusion $\mathcal{J}_j$, which depends mostly on the unresolved velocity fluctuations, is modeled in terms of the temperature gradient. In an isothermal flow, $\mathcal{J}_j$ may be non-zero, and even if the temperature is not constant, there is no reason to couple a term due to mechanical energy gradients to the temperature. A model of the form (??) effectively neglects $\mathcal{J}_j$.

The only attempt to model the SGS turbulent diffusion was that by Knight *et al.* (1998). They argue that $\widetilde{u}_i \simeq \widetilde{\widetilde{u}}_i$ and propose a model of the form

$$\mathcal{J}_j \simeq \widetilde{u}_k \tau_{jk}. \tag{37}$$

A dynamic scale-similar model can be obtained using the generalized central moments (Germano, 1992):

$$\tau(u_i, u_j) = \overline{\rho}\left[\widetilde{u_i u_j} - \widetilde{u}_i\widetilde{u}_j\right] \tag{38}$$

$$\begin{aligned}\tau(u_i, u_j, u_k) = {} & \overline{\rho}\,\widetilde{u_i u_j u_k} - \widetilde{u}_i\tau(u_j, u_k) - \widetilde{u}_j\tau(u_i, u_k) \\ & -\widetilde{u}_k\tau(u_i, u_j) - \overline{\rho}\,\widetilde{u}_i\widetilde{u}_j\widetilde{u}_k.\end{aligned} \tag{39}$$

Using this notation the turbulent diffusion term can be written as

$$2\mathcal{J}_j = \tau(u_j, u_k, u_k) + 2\widetilde{u}_k\tau(u_j, u_k), \tag{40}$$

since $\tau(u_j, u_k) = \tau_{jk}$. Using this formalism, scale-similar models can be derived by approximating the quadratic terms using the filtered velocities $\widetilde{u}_j$ to replace the velocities u_j; for

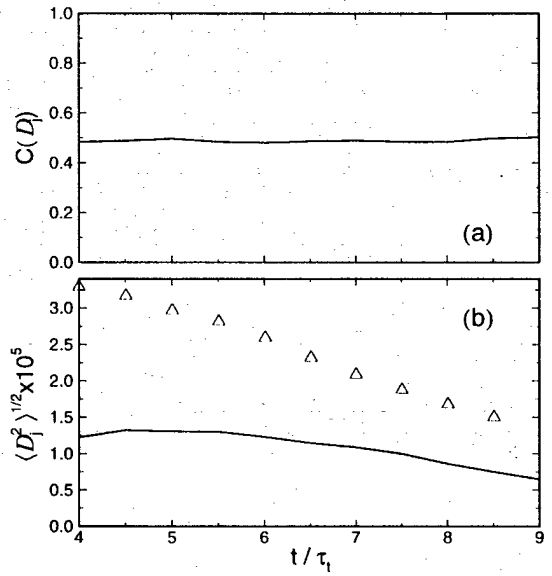

Figure 11: *A priori* comparison of the SGS viscous diffusion $\mathcal{D}_j$. (a) Correlation coefficient and (b) non-dimensional rms magnitude. —— scale-similar model: Δ DNS.

rms magnitude of $\mathcal{J}_j$ (Fig. 10b). When the one-coefficient, scale-similar model is used this over-prediction is significantly reduced. Both models perform equally well for $\overline{\Delta}/\Delta \leq 16$, while neither is accurate for $\overline{\Delta}/\Delta = 32$.

5.4 SGS viscous diffusion

The SGS viscous diffusion $\partial \mathcal{D}_j / \partial x_j$ is the smallest of the terms in the total energy equation, and is about 5% of the divergence of Q_j. No model for this term has been proposed in the literature to date. One possibility is to parameterize it using a scale-similar model of the

form

$$\mathcal{D}_j = C_D(\widetilde{\widetilde{\sigma}_{ij}\tilde{u}_i} - \tilde{\tilde{\sigma}}_{ij}\tilde{\tilde{u}}_i), \tag{48}$$

in which the coefficient can be obtained from

$$C_D = \frac{\left\langle \left[\widetilde{\frac{\overline{\rho}\sigma_{ij}}{\overline{\rho}}\frac{\overline{\rho}u_i}{\overline{\rho}}} - \frac{\widetilde{\overline{\rho}\sigma_{ij}}}{\tilde{\overline{\rho}}}\frac{\widetilde{\overline{\rho}u_i}}{\tilde{\overline{\rho}}} \right] \mathcal{R}_l \right\rangle}{\langle \mathcal{R}_k \mathcal{R}_k \rangle}, \tag{49}$$

where

$$\mathcal{R}_l = \left(\widetilde{\tilde{\sigma}_{lk}\tilde{u}_k} - \tilde{\tilde{\sigma}}_{lk}\tilde{\tilde{u}}_k \right) - \left(\widetilde{\tilde{\sigma}_{lk}\tilde{u}_k} - \tilde{\tilde{\sigma}}_{lk}\tilde{\tilde{u}}_k \right). \tag{50}$$

As can be seen from Fig. 11, this model gives a poor correlation and poor agreement for the prediction of the rms magnitude. However, since the viscous diffusion is relatively small, its contribution to the total energy spectrum does not go to the inertial range, but rather to the decaying range. In this situation the accuracy of the model is degraded, as shown by Meneveau and Lund (1997). Thus, the scale-similar approach may still give good predictions when this term is significant. In this particular flow, the error given by the model (or by not using a model) may be tolerable given the small contribution that the term gives to the energy budget.

6 Conclusions

Several mixed and eddy-viscosity models for the momentum and energy equations have been tested. The velocity, pressure, density and temperature fields obtained from the DNS of homogeneous isotropic turbulence at $Re_\lambda = 50$, $M_t = 0.52$ were filtered and the unclosed terms in the momentum, internal energy and total energy equations were computed.

In the momentum equation, mixed models were found to give better prediction, in terms of both correlation and *rms* amplitude, than the pure eddy-viscosity models. The dynamic adjustment of the model coefficient was beneficial, as already observed by Moin *et al.* (1991).

coefficients in the viscous range of turbulence. *Phys. Fluids* **9**, 3932-3934.

Moin, P., Squires, K. D., Cabot, W. H., and Lee, S. (1991). A dynamic subgrid-scale model for compressible turbulence and scalar transport. *Phys. Fluids A* **3**, 2746-2757.

Normand, X., and Lesieur, M. (1992). Direct and large-eddy simulation of laminar breakdown in high-speed axisymmetric boundary layers. *Theoret. Comput. Fluid Dyn.* **3**, 231-252.

Ristorcelli, J.R., and Blaisdell, G.A. (1997). Consistent initial conditions for the DNS of compressible turbulence. *Phys. Fluids*, **9**, 4-6.

Smagorinsky, J. (1963) General Circulation Experiments with the Primitive Equations. I. The Basic Experiment *Monthly Weather Review* **91**, 99-164.

Speziale, C.G., Erlebacher, G., Zang, T.A., and Hussaini, M.Y. (1988) The subgrid-scale modeling of compressible turbulence. *Phys. Fluids A* **31**, 940-942.

Vreman, B., Geurts, B., and Kuerten, H. (1995a). A priori tests of large eddy simulation of the compressible mixing layer. *J. Eng. Math.* **29**, 299-327.

Vreman, B., Geurts, B., and Kuerten, H. (1995b). Subgrid-modeling in LES of compressible flow. *Applied Sci. Res.* **54**, 191-203.

Yoshizawa, A. (1986). Statistical theory for compressible turbulent shear flows, with the application to subgrid modeling. *Phys. Fluids A* **29**, 2152-2164.

Zang, T. A., Dahlburg, R. B., and Dahlburg, J. P. (1992). Direct and large-eddy simulations of three-dimensional compressible Navier-Stokes turbulence. *Phys. Fluids A* **4**, 127-140.

Multi-Block Large-Eddy Simulations of Turbulent Boundary Layers

Andrea Pascarelli, Ugo Piomelli

Department of Mechanical Engineering
University of Maryland
College Park, MD 20742

and Graham V. Candler

Department of Aerospace Engineering and Mechanics
University of Minnesota
Minneapolis, MN

Submitted to
Journal of Computational Physics
December 18, 1998

Key Words:

Large Eddy Simulation of Turbulence

Block-Structured Mesh

Turbulent Boundary Layer

Subject Classification:

65M06 Finite difference methods

76F99 Turbulence; Other.

Corresponding Author:

Ugo Piomelli
Department of Mechanical Engineering
University of Maryland
College Park, MD 20742

Tel. +1 301 405 5254
Fax +1 301 314 9477
email ugo@eng.umd.edu

near-wall region [2]. The highly irregular interface between the turbulent and non-turbulent flow exhibits three-dimensional bulges on the scale of δ both in the streamwise and spanwise directions, and narrow entrainment eddies, as observed by Robinson [1].

The different length scales of the turbulent eddies in the inner and outer layers can pose a significant challenge for numerical simulations that resolve the energy-carrying structures, such as direct and large-eddy simulations of turbulence. Chapman [4] and Reynolds [5] studied the grid requirements necessary to resolve the turbulent boundary layer. In the outer layer, the turbulent eddies scale with δ. To resolve such structures it is necessary to use a grid-spacing scaled in outer units, $\Delta x_i/\delta$. The number of grid points required to resolve the outer layer in each direction is $N_i = L_i/\Delta x_i \sim L_i/\delta$ (where L_i is the length of the computational domain). Assuming that the boundary-layer thickness scales like $Re^{-0.2}$ (where $Re = U_\infty \ell/\nu$ is the Reynolds number based on the free-stream velocity, U_∞, and a reference length, ℓ, of the same order as the computational domain size, L_i), it is easy to verify that the total number of grid points required to resolve the outer layer is proportional to $Re^{0.4}$, since $N_1 \sim Re^{0.2}$, $N_2 \sim Re^{0.2}$, and $N_3 \sim Re^0$ [4].

Since the inner-layer structures scale in wall units, the grid spacing in wall units, $\Delta x_i^+ = \Delta x_i u_\tau/\nu$, must be kept constant. This results in a number of points in each direction given by

$$N_i = \frac{L_i}{\Delta x_i} = \frac{\nu}{\Delta x_i u_\tau}\frac{L_i}{\ell}\frac{\ell U_\infty}{\nu}\frac{u_\tau}{U_\infty} = \frac{1}{\Delta x_i^+}\frac{L_i}{\ell} Re\sqrt{\frac{C_f}{2}} \sim Re^{1-\alpha}, \qquad (1)$$

where it is assumed that $C_f \sim Re^{-2\alpha}$. Typical values of α are in the range $\alpha \simeq 0.1 - 0.125$, giving a total number of grid points that scales like $N = N_1 N_2 N_3 \sim Re^{2.6}$.

These scaling arguments dictate the size of computational grids that must be used by numerical simulation methods that resolve the energy-carrying turbulent flow structures. In Direct Numerical Simulations (DNS) all of the relevant structures are resolved, down to the smallest scales of motion, and no modeling is used. In Large-Eddy Simulations (LES), only the energy-carrying structures are computed accurately: the small, subgrid, scales, which are more isotropic and drain energy from the large scales through the cascade process, are

modeled. LES can result in significant savings over DNS, in terms of computational costs, especially when no solid boundaries are present: if the grid size corresponds to a wave-number in the inertial region of the spectrum, the resolution required by LES becomes independent of the Reynolds number. When the energy-carrying structures are Reynolds-number dependent, as is the case in the near-wall region of a boundary layer, the cost of the calculations is again affected by the Reynolds number, and is driven by the inner-layer resolution requirements. Although significant savings can be achieved over DNS, the application of LES to high Reynolds number external flows is still expensive.

One possible approach to bypass this limitation in LES is to model the wall layer entirely. Assuming that the near wall layer is in equilibrium, approximate boundary conditions for the wall stress can be derived using the standard logarithmic law [6, 7, 8]. Balaras *et al.* [9] introduced an alternative approach employing boundary-layer equations in attached channel and duct flows, and Cabot [10] applied this method to the separated flow behind a step. Modeling the wall layer can allow the extension of LES to flows at very high Reynolds numbers, but only at the expense of the added empiricism introduced by the approximate boundary conditions. Thus, wherever wall models do not give sufficient accuracy, the near-wall layer must be resolved.

In computational fluid dynamics there are different ways of discretizing the physical domains. Based on the connectivity, the grids can be classified as structured, unstructured, or multi-block. The most straightforward approach is the structured grid, in which connectivity information is not needed explicitly so that each mesh point is identified by indices, and the neighbors are known. While a structured grid is simple to implement, and allows easy control of the order of accuracy and conservation properties of the scheme, it can result in a large number of points in regions where they are not needed. In a boundary layer, for instance, the spanwise and streamwise spacings need to be nearly constant, to satisfy the inner-layer resolution requirements discussed above. However, in the outer layer the grid spacing specified by the inner-layer resolution requirement results in a grid spacing that is

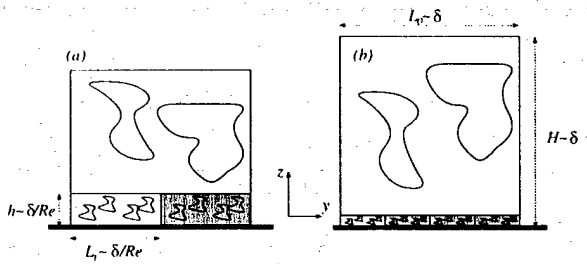

Figure 1: Sketch of the multi-block structure in the cross-plane with "inner-layer units" The flow is out of the paper. (a) Low Reynolds number; (b) high Reynolds number.

a relatively weak function of the Reynolds number, as the size of the ILU remains constant. The interface between the smaller inner-layer domains and the larger outer-layer ones may pose a problem, since the largest eddy present at the interface between layers is determined by the size of the ILU. The non-linear interactions between high wave-numbers will of course generate subharmonic modes, i.e., larger structures, and eventually destroy the periodicity. There will be an adjustment layer in which the flow is still characterized by the periodicity length forced by the inner-layer unit. If the thickness of this layer is small, the proposed approach may be feasible.

As mentioned above, this technique requires the existence of at least one direction of homogeneity in the flow, and it may not be applicable in highly three-dimensional flows. However, there may be a range of intermediate configurations in which one could use periodically repeated inner-layer units in some regions of the flow only. To compute the flow over an airplane wing, for instance, it might be possible to use periodically repeated inner layer units away from strong sources of three-dimensionality (the wing root and tip regions, the engine nacelles etc.). This issue requires further study and is not addressed here.

In this study the multi-block approach is proposed and tested in a wall-bounded flow with one direction of homogeneity, namely a temporally developing boundary layer. This flow was chosen because it contains many of the features of importance in a spatially developing

flow, which is technologically more important, but does not require special treatment of the inflow and outflow conditions. Single block LES calculations were performed at two Mach numbers, and the results are compared with those obtained using the inner-layer unit approach. To separate the errors due to the periodicity of the inner layer from the numerical errors arising from the use of multi-block grids (interpolation, interface between subdomains) the calculations were carried out using an explicit code, with one-to-one correspondence between the domains. Studies of real flows would probably require non-conforming meshes. With the same aim, a well-established subgrid-scale model is used, and no attempt is made to employ more advanced, and perhaps more accurate, models.

In the next section, the problem formulation, numerical method and subgrid-scale model used are described. Then, computational results are presented and discussed. Finally, some conclusions are drawn in the last section.

2 Problem formulation

2.1 Governing equations

The set of differential equations in Cartesian coordinates satisfied by a viscous flow in the absence of body forces reads

$$\frac{\partial \rho}{\partial t} + \frac{\partial}{\partial x_j}(\rho u_j) = 0, \tag{2}$$

$$\frac{\partial \rho u_i}{\partial t} + \frac{\partial}{\partial x_j}(\rho u_j u_i + p\delta_{ji} - \sigma_{ji}) = 0, \tag{3}$$

$$\frac{\partial \rho E}{\partial t} + \frac{\partial}{\partial x_j}[(\rho E + p)\, u_j - \sigma_{ji} u_i + q_j] = 0, \tag{4}$$

where the summation convention applies to repeated indices. Here, ρ is the fluid density, u_j the fluid velocity component in j direction, $E = \epsilon + u_k u_k/2$ is the total energy per unit mass (where $\epsilon = C_v T$ is the internal energy per unit mass, C_v is the specific heat at constant volume and T the temperature), p is the thermodynamic pressure, σ_{ji} is the viscous stress tensor and q_j is the conduction heat flux. In the present work, the fluid is assumed to be an ideal gas with constant specific heats (whose ratio is $\gamma = 1.4$). Thus, the pressure is related

turbulent Mach number of 0.52. In their study, however, the divergence of $\mathcal{J}_j$ was found to be a significant fraction of the divergence of the SGS heat flux: thus, the first assumption may not be justified for high turbulent Mach numbers. In the present simulations, however, the turbulent Mach number is significantly smaller than that examined by Vreman *et al.* [17] and Martín *et al.* [21] (it is of the order of 0.03–0.1), and the present assumption is acceptable to test the validity of the multi-block approach.

2.3 Numerical scheme

The general conservation laws can be expressed as

$$\frac{\partial U}{\partial t} = \mathcal{S}(U) \equiv -\frac{\partial F_j(U)}{\partial x_j}. \tag{19}$$

$U \in \mathbf{R}^5$ is a vector whose components are the independent variables, and $F_j = F_{cj} - F_{dj} \in \mathbf{R}^5$ is the total flux (convective and diffusive) in the x_j direction. They are defined by

$$U = \begin{Bmatrix} \overline{\rho} \\ \overline{\rho}\widetilde{u}_i \\ \overline{\rho}\widetilde{E} \end{Bmatrix}, \quad F_{cj} = \begin{Bmatrix} \overline{\rho}\widetilde{u}_j \\ \overline{\rho}\widetilde{u}_j\widetilde{u}_i + \overline{p}\delta_{ji} \\ \left(\overline{\rho}\widetilde{E} + \overline{p}\right)\widetilde{u}_j \end{Bmatrix}, \quad F_{dj} = \begin{Bmatrix} 0 \\ \tilde{\sigma}_{ji} - \tau_{ji} \\ \tilde{\sigma}_{ji}u_i - \tilde{q}_j - \gamma C_v Q_j \end{Bmatrix}; \tag{20}$$

$\mathcal{S} = \mathcal{S}_c - \mathcal{S}_d$ is the global spatial differential operator. Equation (19) is discretized by approximating U as $U^n_{i,j,k}$ at location $(i\Delta x_1, j\Delta x_2, k\Delta x_3)$ and time $t^n = n\Delta t$, and solved numerically.

To resolve properly the details of the boundary layer, the grid points are clustered near the wall in the wall normal direction (z) while the spacing in x and y is kept uniform. The numerical solutions are computed on a uniform grid in computational space (ξ, η, ζ). The transformation relations from physical space (x, y, z) to the computational space are:

$$x = \xi, \quad y = \eta, \quad z = z(\zeta) \tag{21}$$

and the wall-normal derivatives are computed in the regular ζ-space, *e.g.*,

$$\frac{\partial f}{\partial z} = \frac{\partial f}{\partial \zeta}\frac{d\zeta}{dz}, \quad \frac{\partial^2 f}{\partial z^2} = \frac{\partial f}{\partial \zeta}\frac{d^2\zeta}{dz^2} + \frac{\partial^2 f}{\partial \zeta^2}\left(\frac{d\zeta}{dz}\right)^2, \quad \text{etc.}$$

The Favre-filtered Navier-Stokes equations (10–12) thus become

$$\frac{\partial U}{\partial t} + \frac{\partial F}{\partial \xi} + \frac{\partial G}{\partial \eta} + \frac{\partial H}{\partial \zeta}\frac{d\zeta}{dz} - \frac{\partial F_d}{\partial \xi} - \frac{\partial G_d}{\partial \eta} - \frac{\partial H_d}{\partial \zeta}\frac{d\zeta}{dz} = 0 \tag{22}$$

where $F = F_{c1}$, $G = F_{c2}$, $H = F_{c3}$, and a similar notation is used for the diffusive fluxes.

Let L_x, L_y, L_z be the dimensions of the computational domain Ω in the x, y, z directions respectively. For the discretization of Ω, let

$$\begin{aligned} x_i &= \xi_i \Delta x \qquad (\xi_i = i-1), \quad i = 1, \ldots, nx \\ y_i &= \eta_j \Delta y \qquad (\eta_j = j-1), \quad j = 1, \ldots, ny \\ z_1 = 0, \quad z_k &= \frac{1-\alpha^{\zeta_k}}{1-\alpha}\Delta z_1 \quad (\zeta_k = k-1), \quad k = 2, \ldots, nz \end{aligned}$$

where $\Delta x = L_x/(nx-1)$, $\Delta y = L_y/(ny-1)$ and nx, ny are the number of grid points in the x, y directions, respectively. A Cartesian non-uniform grid with nz points stretched with geometric progression in wall-normal direction is used. $\alpha = \frac{\Delta z_{k+1}}{\Delta z_k}$ is the constant ratio of successive intervals (*stretching factor*), with $\Delta z_k = z_{k+1} - z_k$.

The numerical approximation to the spatial operator $\mathcal{S}_c(u)$ is

$$S_c(u) = -\left[\left.\frac{\delta F}{\delta x}\right|_{i,j,k} + \left.\frac{\delta G}{\delta y}\right|_{i,j,k} + \left.\frac{\delta H}{\delta z}\right|_{i,j,k}\left(\frac{d\zeta}{dz}\right)_{z=z_k}\right] \tag{23}$$

where $\delta f/\delta x_l$ denote a finite difference operator acting on f with respect to x_l.

The approximation of the convective flux derivatives in the Navier-Stokes equations is a key element of the spatial integration. Here, the discrete operator calculations are independent in x, y and z directions. For example, $\delta F/\delta x|_{i,j,k}$ is calculated component-wise holding indices j and k fixed, *i.e.*, along a slice of data in x-direction. A fourth-order accurate scheme is used, according to which the first derivative is constructed as the weighted sum of a central-difference method and an upwind-biased method. This approach yields a scheme with good modified wavenumber performance and a small level of dissipation at high wavenumbers. The x–direction derivative is given by

$$\left.\frac{\delta F}{\delta x}\right|_{i,j,k} = \frac{1}{\Delta x}\left[\frac{1}{180}\left(F_{i+2,j,k} - F_{i-2,j,k}\right) - \frac{2}{9}\left(F_{i+1,j,k} - F_{i-1,j,k}\right) + \frac{64}{45}\left(F_{i+\frac{1}{2},j,k} - F_{i-\frac{1}{2},j,k}\right)\right], \tag{24}$$

a second-order-accurate formula. At the top of the domain, the normal gradients of the conserved variables were set to zero.

The use of periodic boundary conditions implies that the boundary layer develops in time, rather than in the streamwise direction. To simulate properly a spatially developing boundary layer, either inflow-outflow conditions must be used, or some other approximate technique, such as the "fringe method" [24] must be adopted. Since the purpose of the present calculation is to test the ILU concept, it was preferred not to introduce additional uncertainties. Although this configuration is not the exact equivalent of a flat-plate boundary layer, it contains many of the important physical features of that flow (inner- and outer-layer scalings, for instance). Thus, it constitutes a consistent test-case for the comparison of single- and multi-block calculations.

2.5 Block partitioning and grid distribution

Two types of calculations were performed: first, single-block computations were carried out as baseline cases; then, multi-block computations were performed to validate the proposed approach. In the single-block cases, 64×48×48 grid points were used in the streamwise, spanwise and wall-normal directions, respectively, to discretize a domain whose size was equal to that of the initial field ($120\delta_o^* \times 30\delta_o^* \times 22\delta_o^*$); this resulted in an initial grid resolution $\Delta x^+_o \approx 103$, $\Delta y_o^+ \approx 34$, and $\Delta z^+_{min,o} = 0.15$ (a subscript "o" indicates that the initial friction velocity, $u_{\tau,o}$, and displacement thickness, δ_o^*, were used for the normalizations).

The multi-block calculations were carried out using the arrangement shown in Fig. 2. Three rectangular subdomains were used, with conforming grids (the grid lines were continuous across the interfaces). Interface and boundary conditions were specified by using four "ghost points" to ensure that fourth-order accuracy was achieved even at the sub-domain interfaces.

The inner layer was discretized using two subdomains, Blocks 1 and (1) in Fig. 2: the latter is purely virtual, and is periodic copy of Block 1. The inner-layer unit had the same

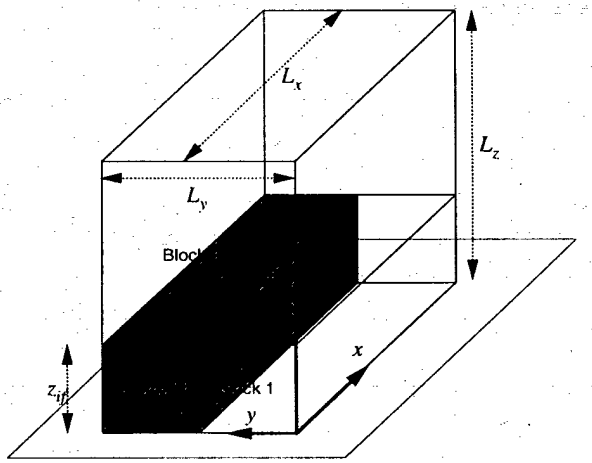

Figure 2: Multi-block arrangement for 3D turbulent boundary layer

dimension in the streamwise direction as the single-block calculation, and extended up to a height z_{if}, which could be varied. Its spanwise size was $L^+_{y,o} = 820$. The dimensions of the ILU were significantly larger than those of the "minimal flow unit" of Jimenez and Moin [13], and were sufficient to contain several near-wall structures. The outer layer was discretized using a single block (Block 2 in the figure), whose dimensions were $L^+_{x,o} = 6570$, $L^+_{y,o} = 1640$; in the wall normal direction, it extended from z^+_{if} to $L^+_{z,o} = 1230$. Two values of z_{if} were tested: in one case, the interface was placed in the buffer region, at $z_o^+ = 30$, in the other, in the logarithmic layer at $z_o^+ = 104$. The grids used for the two cases are summarized in Table 1.

	$z_o^+ = 30$	$z_o^+ = 104$
Inner layer	64×24×24	64×24×32
Outer layer	64×48×24	64×48×16

Table 1: Grid resolutions.

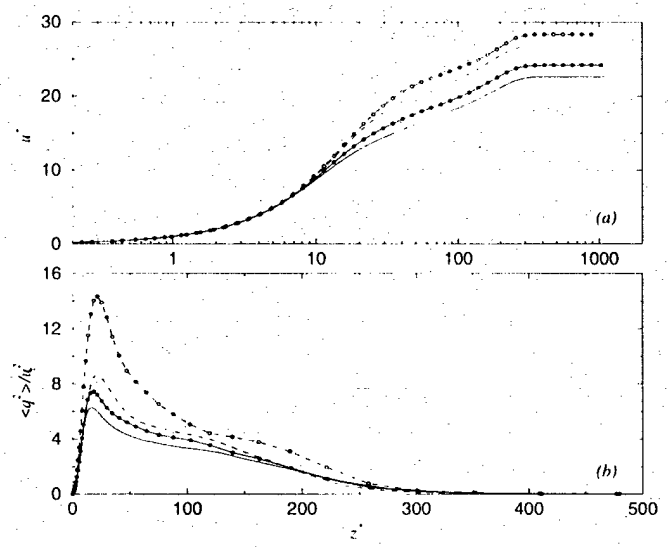

Figure 4: Mean velocity profiles and trace of the resolved Reynolds stresses. Lines: $M = 0.3$; lines with symbols: $M = 0.7$. —— $tu_{\tau,o}/\delta_o^* = 0.4$; --- $tu_{\tau,o}/\delta_o^* = 2$.

thus, the Reynolds number based on u_τ and ν ranged from 1110 to 890 for the low Mach number case, and from 410 to 940 in the high Mach number calculation.

Figure 4 shows the profiles of the plane-averaged mean velocity, $u^+ = \langle u \rangle / u_\tau$ and trace of the resolved Reynolds stresses, $\langle q^2 \rangle = \langle u_i'' u_i'' \rangle$ (where $u_i'' = \widetilde{u}_i - \langle \widetilde{u}_i \rangle$ and $\langle \cdot \rangle$ indicates an average over the two homogeneous directions) obtained from the single-block calculation after 0.4 and 2 LETOTs. The instantaneous friction velocity is used to normalize both quantities. A well-defined logarithmic layer is observed in both cases, although its intercept is higher (approximately 7, instead of the standard value of 5.2) due to the low resolution used, which results in an overestimation of the thickness of the wall layer, and in a lower value of the wall stress τ_w. Correspondingly, high values of $\langle q^2 \rangle$ are observed

Case	M	$z^+_{1,l,o}$	Parameters
003	0.3		Single block
103	0.3	30	Thick transition ($\beta = 15$)
203	0.3	30	Thin transition ($\beta = 90$)
303	0.3	30	Thin transition ($\beta = 90$), random noise correction
403	0.3	104	Thin transition ($\beta = 90$), random noise correction
007	0.7		Single block
307	0.7	30	Thin transition ($\beta = 90$), random noise correction

Table 2: Summary of simulation parameters.

Several multi-block calculations, whose parameters are summarized in Table 2, were compared with the single-block calculations. The multi-block calculations differed by the height of the interface between the two layers, and by the thickness of the transition layer (*i.e.*, by the parameter β). In addition, in two of the calculations the initial condition was modified by adding a random noise component to match the initial plane-averaged Reynolds stress distribution. The weighted-average procedure described in Section 2.4 results in a defect in the plane-averaged Reynolds stresses equal to

$$\Delta\langle u_i'' u_j'' \rangle = 2g(z)[1 - g(z)]\langle u_i'' u_j'' \rangle. \tag{35}$$

To correct this defect, a procedure similar to that used by Lund *et al.* [25] to generate inflow conditions for spatially developing simulations was followed. At each vertical location, three sequences of random numbers with zero mean, unit variance, and zero covariance with the other two distributions were generated. These uncorrelated random fluctuations were then scaled and combined to match $\Delta\langle u_i'' u_j'' \rangle$. The resulting signals were added to each component of the velocity field. This procedure has two effects: first, it gives an initial condition whose second-order statistics match exactly those of the single-block calculation; secondly, the random fluctuation scrambles somewhat the initial periodicity of the flow at the interface; this was expected to be beneficial in decreasing the thickness of the transition layer. As will be shown later, this correction proved ineffectual because the uncorrelated random noise was rapidly dissipated.

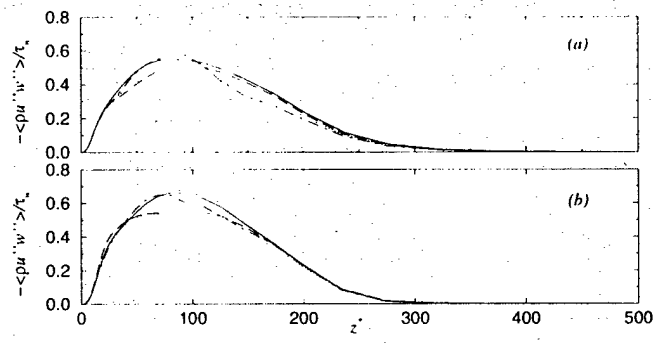

Figure 8: Resolved Reynolds shear stress for $M = 0.3$. (a) $tu_\tau/\delta^* = 0.4$; (b) $tu_\tau/\delta^* = 2$. —— Single block; - - - $z^+_{if,o} \approx 30$, wide transition; --- $z^+_{if,o} \approx 30$, narrow transition; —-- $z^+_{if,o} \approx 104$ narrow transition.

with and without random noise give the same results, as shown in Fig 7.

The resolved Reynolds shear stress, $-\langle \rho u'' w'' \rangle$ normalized by τ_w is shown in Fig. 8 for the $M = 0.3$ calculation. The differences observed in the rms intensities are more evident here. The calculations in which the interface is in the buffer layer under-predict the stress throughout the buffer and logarithmic regions; more accurate prediction of the stresses is obtained when the interface is in the logarithmic region.

At the higher Mach number, similar results are obtained. However, the agreement is better, even for an interface in the buffer layer. This result may be due to the fact that at higher Mach number the convection effects are more significant, and stronger non-linear interactions scramble the initial periodicity more rapidly.

The first- and second-order statistics obtained using the multi-block approach with a periodic inner-layer unit compare well with those of single-block calculations at both Mach numbers examined. The main effect of the interface on the results is due to the initialization procedure, which results in a Reynolds-stress defect that was not recovered by the time the

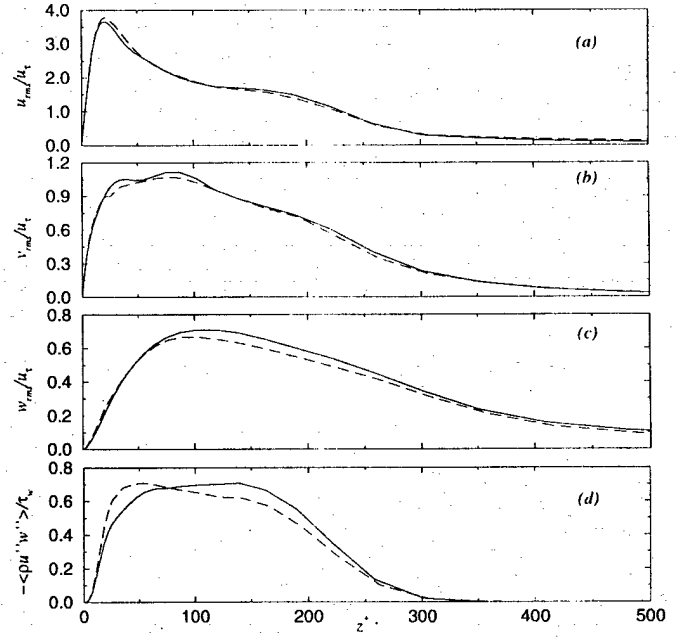

Figure 9: Turbulence intensities and Reynolds shear stress at $tu_{\tau,o}/\delta^*_o = 2$ and $M = 0.7$. (a) Streamwise rms, (b) spanwise rms, (c) wall normal rms, (d) Reynolds shear stress. —— Single block; ——— $z^+_{if,o} \approx 30$, narrow transition.

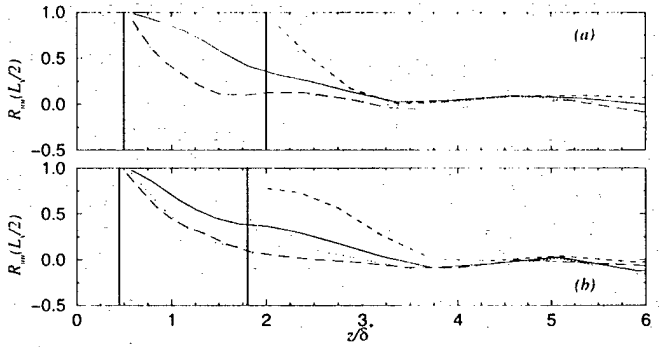

Figure 11: Two-point spatial autocorrelation function $R_{uu}(L_y/2)$. (a) $tu_\tau/\delta^* = 0.4$, (b) $tu_\tau/\delta^* = 2$. —— $z^+_{if,o} \approx 30$, wide transition, $M = 0.3$; · · · · $z^+_{if,o} \approx 30$, narrow transition, $M = 0.3$; - - - $z^+_{if,o} \approx 104$, narrow transition, $M = 0.3$; — — — $z^+_{if,o} \approx 30$, narrow transition, $M = 0.7$. The thick lines represent the two interfaces.

of the fluid-dynamic variables. In Figs. 12 and 13 the velocity contours are shown for the two values of the interface location. It is quite remarkable to observe the difference in the structures between the two halves of the domain. The large structure observed in the v contours at $y/\delta^* \approx 15$ and $z/\delta^* \approx 4$ in Fig. 13b is one example of a completely asymmetric eddy which must obviously result from the nonlinear interactions that occur above the interface. Also notice that the high- and low-interface simulations were started from the same initial conditions; thus one would expect a similar distribution of the turbulent eddies at corresponding times. Such is the case; if Figs. 12 and 13 are compared, the large structures appear to be located at roughly at the place and have similar strength. For the different interfaces, some temporal decorrelation is caused by the modification of the initial condition. In an unstable flow such as this one, small differences in the initial conditions are amplified, and eventually lead to a complete loss of correlation. However, the statistics should not be affected, as is the case in the present calculation.

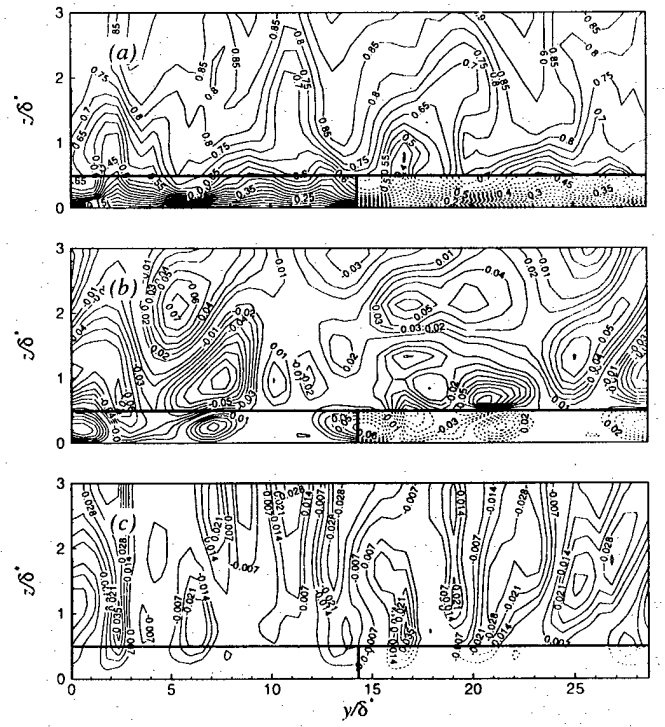

Figure 12: Instantaneous velocity iso-contours for $M = 0.3$, $tu_\tau/\delta^* = 1$. $z^+_{if,o} \approx 30$, thin transition. (a) u; (b) v; (c) w. Dashed lines: virtual block.

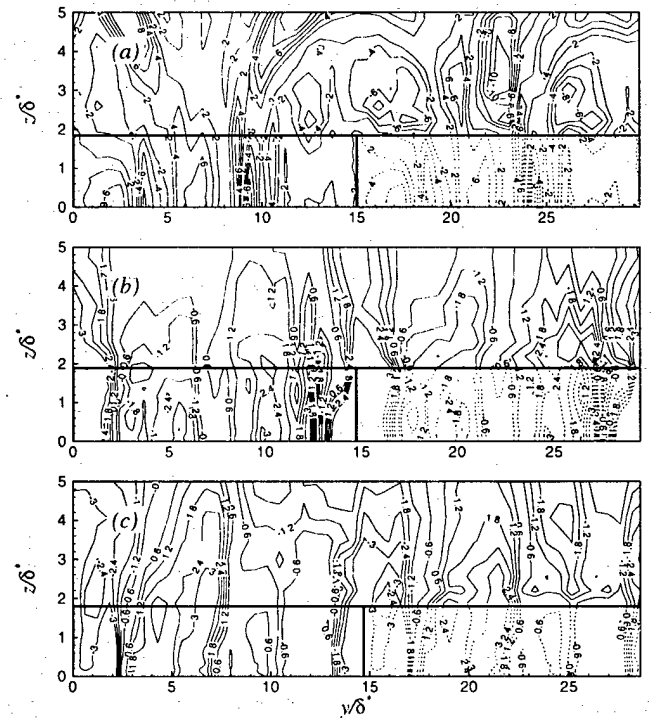

Figure 14: Time sequence of the iso-contours of the pressure fluctuations (normalized by τ_w) for $M = 0.3$. $z^+_{tf,o} \approx 104$, thin transition. (a) $tu_\tau/\delta^* = 0.01$; (b) $tu_\tau/\delta^* = 0.4$; (c) $tu_\tau/\delta^* = 1$. Dashed lines: virtual block.

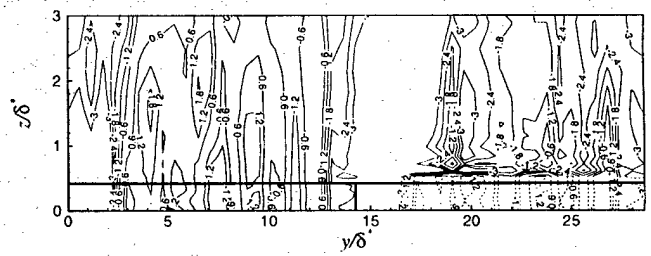

Figure 15: Iso-contours of the pressure fluctuations (normalized by τ_w) at $tu_\tau/\delta^* = 1$. $M = 0.3$, $z^+_{tf,o} \approx 30$, thin transition. Dashed lines: virtual block.

Multi-block simulations with an ILU that is extended periodically give good agreement with single-block calculations for first- and second-order statistics, especially if the interface is located in the logarithmic layer. Placing the interface in the buffer layer, where much of the turbulent activity takes place, results in under-prediction of the Reynolds stress magnitudes and spurious pressure fluctuations. The periodicity introduced at the interface between the inner and outer layers does not spread outwards. Within a few grid points, larger structures are generated, and the correlation between the two halves of the domain is lost.

In the present study, only modest computational savings were achieved: the two multi-block calculations required only 25 and 33% fewer points than the single-block calculation. However with increased Reynolds number, the ratio of the near-wall periodic region thickness to the boundary-layer thickness decreases; this results in a dramatic increase in the number of grid points required to resolve the near wall region with a conventional method. With the present approach, the cost does not increase as rapidly since the ILU can be repeated as many times as necessary in the spanwise direction. If non-conforming meshes are used, such that the spanwise and streamwise spacings of the outer-layers can be increased over those of the inner-layer sub-domain, additional savings can be achieved.

[20] P. Moin, K. D. Squires, W. H. Cabot, and S. Lee. "A dynamic subgrid-scale model for compressible turbulence and scalar transport." *Phys. Fluids A* **3**, 2746 (1991).

[21] M. P. Martin, U. Piomelli, and G. Candler. "Subgrid-scale models for compressible large-eddy simulations." In *Proc. 1999 ASME Symposium on Transitional and Turbulent Compressible Flow* (1999).

[22] J. L. Steger, and R. F. Warming. "Flux vector splitting of the inviscid gasdynamic equation with application to finite difference methods." *J. Comput. Phys.* **40**, 263 (1981).

[23] J. H. Williamson. "Low-Storage Runge-Kutta Schemes." *J. Comput. Phys.* **35**, 48 (1980).

[24] P. R. Spalart and J. H. Watmuff. "Experimental and numerical study of a turbulent boundary layer with pressure gradients." *J. Fluid Mech.* **249**, 337 (1993).

[25] T. S. Lund, X. Wu, and K. D. Squires. "Generation of turbulent inflow data for spatially-developing boundary layer simulations." *J. Comput. Phys.* **140**, 233 (1998).

Subgrid-Scale Models for Compressible Large-Eddy Simulations

M. Pino Martín[1]

Department of Aerospace Engineering and Mechanics

University of Minnesota

110 Union St. SE. Minneapolis, MN 55455

pino@aem.umn.edu / Fax: 612-626-1596

Ugo Piomelli

Department of Mechanical Engineering

University of Maryland

College Park, MD 20742

ugo@eng.umd.edu / Fax: 301-314-9477

Graham V. Candler

Department of Aerospace Engineering and Mechanics

University of Minnesota

110 Union St. SE, Minneapolis, MN 55455

candler@aem.umn.edu / Fax: 612-626-1558

[1]Corresponding author.

Abstract

An *a priori* study of subgrid-scale models for the unclosed terms in the energy equation is carried out using the flow field obtained from the direct simulation of homogeneous isotropic turbulence. Scale-similar models involve multiple filtering operations to identify the smallest resolved scales that have been shown to be the most active in the interaction with the unresolved subgrid scales (SGS). In the present study these models are found to give more accurate prediction of the SGS stresses and heat fluxes than eddy-viscosity and eddy-diffusivity models, as well as improve prediction of the SGS turbulent diffusion, SGS viscous dissipation, and SGS viscous diffusion.

Submitted to "Theoretical & Computational Fluid Dynamics", 1999

2 Governing equations

To obtain the equations governing the motion of the resolved eddies, we must separate the large from the small scales. LES is based on the definition of a filtering operation: a resolved variable, denoted by an overbar, is defined as (Leonard, 1974)

$$\overline{f}(\mathbf{x}) = \int_D f(\mathbf{x}')G(\mathbf{x}, \mathbf{x}'; \overline{\Delta})d\mathbf{x}'. \tag{1}$$

where D is the entire domain and G is the filter function, and $\overline{\Delta}$ is the filter-width associated with the wavelength of the smallest scale retained by the filtering operation. Thus, the filter function determines the size and structure of the small scales.

In compressible flows, it is convenient to use Favre-filtering (Favre, 1965a,b) to avoid the introduction of subgrid scale terms in the equation of conservation of mass. A Favre-filtered variable is defined as $\widetilde{f} = \overline{\rho f}/\overline{\rho}$. In addition to the mass and momentum equations, one can choose solving an equation for the internal energy, enthalpy or total energy. Applying the Favre-filtering operation, we obtain the resolved transport equations

$$\frac{\partial \overline{\rho}}{\partial t} + \frac{\partial}{\partial x_j}\left(\overline{\rho}\,\widetilde{u}_j\right) = 0. \tag{2}$$

$$\frac{\partial \overline{\rho}\,\widetilde{u}_i}{\partial t} + \frac{\partial}{\partial x_j}\left(\overline{\rho}\,\widetilde{u}_i\widetilde{u}_j + \overline{p}\delta_{ij} - \widetilde{\sigma}_{ji}\right) = -\frac{\partial \tau_{ji}}{\partial x_j}. \tag{3}$$

$$\frac{\partial(\overline{\rho}\,\widetilde{e})}{\partial t} + \frac{\partial}{\partial x_j}\left(\overline{\rho}\,\widetilde{u}_j\widetilde{e}\right) + \frac{\partial \widetilde{q}_j}{\partial x_j} + \overline{p}\widetilde{S}_{kk} - \widetilde{\sigma}_{ji}\widetilde{S}_{ij} = -C_v\frac{\partial Q_j}{\partial x_j} - \Pi_{dil} + \epsilon_v. \tag{4}$$

$$\frac{\partial(\overline{\rho}\,\widetilde{h})}{\partial t} + \frac{\partial}{\partial x_j}\left(\overline{\rho}\,\widetilde{u}_j\widetilde{h}\right) + \frac{\partial \widetilde{q}_j}{\partial x_j} - \frac{\partial \overline{p}}{\partial t} - \widetilde{u}_j\frac{\partial \overline{p}}{\partial x_j} - \widetilde{\sigma}_{ji}\widetilde{S}_{ij} = -C_v\frac{\partial Q_j}{\partial x_j} - \Pi_{dil} + \epsilon_v. \tag{5}$$

$$\frac{\partial}{\partial t}(\overline{\rho}\,\widetilde{E}) + \frac{\partial}{\partial x_j}\left[(\overline{\rho}\,\widetilde{E} + \overline{p})\widetilde{u}_j + \widetilde{q}_j - \widetilde{\sigma}_{ji}\widetilde{u}_i\right] = -\frac{\partial}{\partial x_j}\left(\gamma C_v Q_j + \frac{1}{2}\mathcal{J}_j - \mathcal{D}_j\right). \tag{6}$$

Here ρ is the density, u_j is the velocity in the x_j direction, p the pressure, $\epsilon = c_vT$ is the internal energy per unit mass, T the temperature; $h = \epsilon + p/\rho$ is the enthalpy per unit mass;

$E = \epsilon + u_iu_i/2$ is the total energy per unit mass, and the diffusive fluxes are given by

$$\widetilde{\sigma}_{ij} = 2\widetilde{\mu}\widetilde{S}_{ij} - \frac{2}{3}\widetilde{\mu}\delta_{ij}\widetilde{S}_{kk}, \qquad \widetilde{q}_j = -\widetilde{k}\frac{\partial \widetilde{T}}{\partial x_j}, \tag{7}$$

where $S_{ij} = (\partial u_i/\partial x_j + \partial u_j/\partial x_i)$ is the strain rate tensor, and $\widetilde{\mu}$ and $\widetilde{k}$ are the viscosity and thermal conductivity corresponding to the filtered temperature $\widetilde{T}$.

The effect of the subgrid scales appears on the right hand side of the governing equations through the SGS stresses τ_{ij}; SGS heat flux Q_j; SGS pressure-dilatation Π_{dil}; SGS viscous dissipation ϵ_v; SGS turbulent diffusion $\partial\mathcal{J}_j/\partial x_j$; and SGS viscous diffusion $\partial\mathcal{D}_j/\partial x_j$. These quantities are defined as:

$$\tau_{ij} = \overline{\rho}\left(\widetilde{u_iu_j} - \widetilde{u}_i\widetilde{u}_j\right) \tag{8}$$

$$Q_j = \overline{\rho}\left(\widetilde{u_jT} - \widetilde{u}_j\widetilde{T}\right) \tag{9}$$

$$\Pi_{dil} = \overline{pS_{kk}} - \overline{p}\widetilde{S}_{kk} \tag{10}$$

$$\epsilon_v = \overline{\sigma_{ji}S_{ij}} - \widetilde{\sigma}_{ji}\widetilde{S}_{ij} \tag{11}$$

$$\mathcal{J}_j = \overline{\rho}\left(\widetilde{u_ju_ku_k} - \widetilde{u}_j\widetilde{u_ku_k}\right) \tag{12}$$

$$\mathcal{D}_j = \overline{\sigma_{ji}u_i} - \widetilde{\sigma}_{ji}\widetilde{u}_i. \tag{13}$$

The equation of state has been used to express pressure-gradient and pressure-diffusion correlations in terms of Q_j and Π_{dil}. It is also assumed that $\overline{\mu(T)S_{ij}} \simeq \mu(\widetilde{T})\widetilde{S}_{ij}$, and that an equivalent equality involving the thermal conductivity applies. Vreman *et al.* (1995b) performed *a priori* tests using DNS data obtained from the calculation of a mixing layer at Mach numbers in the range 0.2–0.6, and concluded that neglecting the nonlinearities of the diffusion terms in the momentum and energy equations is acceptable.

3 *A priori* test

One method to evaluate the performance of models for LES or RANS calculations is the *a priori* test, in which the velocity fields obtained from a direct simulation are filtered to

τ_{kk} is modeled separately:

$$\tau_{ij} - \frac{\delta_{ij}}{3}\tau_{kk} = -C_s^2 2\overline{\Delta}^2\overline{\rho}\,|\tilde{S}|\left(\tilde{S}_{ij} - \frac{\delta_{ij}}{3}\tilde{S}_{kk}\right) = C_s\alpha_{ij}; \qquad \tau_{kk} = C_I 2\overline{\rho}\,\overline{\Delta}^2|\tilde{S}|^2 = C_I\alpha \quad (16)$$

with $C_s = 0.16$ and $C_I = 0.09$.

Moin *et al.* (1991) proposed a modification of the eddy-viscosity model (16) in which the two model coefficients were determined dynamically, rather than input *a priori*, using the Germano identity $\mathcal{L}_{ij} = T_{ij} - \widehat{\tau_{ij}}$ (Germano, 1992), which relates the subgrid-scale stresses τ_{ij} to the "resolved turbulent stresses" $\mathcal{L}_{ij} = \left(\widehat{\overline{\rho u_i}\,\overline{\rho u_j}}/\overline{\rho}\right) - \widehat{\overline{\rho u_i}}\,\widehat{\overline{\rho u_j}}/\widehat{\overline{\rho}}$, and the subtest stresses $T_{ij} = \widehat{\overline{\rho}}\,\widehat{u_i u_j} - \widehat{\overline{\rho}}\,\tilde{\hat{u}}_i\tilde{\hat{u}}_j$ (where $\tilde{\hat{f}} = \widehat{\overline{\rho} f}/\widehat{\overline{\rho}}$, and the hat represents the application of the test filter $\widehat{G}$ of characteristic width $\widehat{\Delta} = 2\overline{\Delta}$) that appear if the filter $\widehat{G}$ is applied to (3). Moin *et al.* (1991) determined the model coefficients by substituting (16) into the Germano identity and contracting with $\tilde{S}_{ij}$. In the present paper the contraction proposed by Lilly (1992) to minimize the error in a least-squares sense will be used instead. Accordingly, the two model coefficients for the Dynamic Eddy-Viscosity model (DEV) will be given by

$$C = C_s^2 = \frac{\langle \mathcal{L}_{ij} M_{ij}\rangle}{\langle M_{kl} M_{kl}\rangle}; \qquad C_I = \frac{\langle \mathcal{L}_{kk}\rangle}{\langle\beta - \widehat{\alpha}\rangle}, \quad (17)$$

where $\beta_{ij} = -2\widehat{\Delta}^2\widehat{\overline{\rho}}\,|\tilde{\hat{S}}|(\tilde{\hat{S}}_{ij} - \delta_{ij}\tilde{\hat{S}}_{kk}/3)$, $M_{ij} = \beta_{ij} - \widehat{\alpha_{ij}}$, $\beta = 2\widehat{\Delta}^2\widehat{\overline{\rho}}\,|\tilde{\hat{S}}|^2$.

Scale-similar models are based on the assumption that the most active subgrid scales are those closer to the cutoff, and that the scales with which they interact are those right above the cutoff wavenumber (Bardina *et al.*, 1980). Thus, scale-similar models employ multiple operations to identify the smallest resolved scales and use the smallest "resolved" stresses to represent the SGS stresses. Although these models account for the local energy events, they underestimate the dissipation.

Speziale *et al.* (1988) proposed the addition of a scale-similar part to the eddy-viscosity model of Yoshizawa (1986) introducing the mixed model. In this way, the eddy-viscosity contribution provides the dissipation that is underestimated by purely scale-similar models.

This mixed model was also used by Erlebacher *et al.* (1992) and Zang *et al.* (1992), and is given by

$$\tau_{ij} - \frac{\delta_{ij}}{3}\tau_{kk} = C_s\alpha_{ij} + A_{ij} - \frac{\delta_{ij}}{3}A_{kk}; \qquad \tau_{kk} = C_I\alpha + A_{kk}, \quad (18)$$

where $A_{ij} = \overline{\rho}\,(\widetilde{\widetilde{u}_i\widetilde{u}_j} - \tilde{\widetilde{u}}_i\tilde{\widetilde{u}}_j)$.

Erlebacher *et al.* (1992) tested the constant coefficient model *a priori* and by comparing DNS and LES results of compressible isotropic turbulence and found good agreement in the dilatational statistics of the flow, as well as high correlation between the exact and the modeled stresses. Zang *et al.* (1992) compared the DNS and LES results of isotropic turbulence with various initial ratios of compressible to total kinetic energy. They obtained good agreement for the evolution of quantities such as compressible kinetic energy and fluctuations of the thermodynamic variables.

Dynamic model adjustment can be also applied to the mixed model (18), to yield the Dynamic Mixed Model (DMM)

$$C = \frac{\langle \mathcal{L}_{ij} M_{ij}\rangle - \langle N_{ij} M_{ij}\rangle}{\langle M_{lk} M_{lk}\rangle}; \qquad C_I = \frac{\langle \mathcal{L}_{kk} - N_{kk}\rangle}{\langle\beta - \widehat{\alpha}\rangle}, \quad (19)$$

with $B_{ij} = \widehat{\overline{\rho}}\,(\tilde{\hat{\tilde{u}}}_i\tilde{\hat{\tilde{u}}}_j - \tilde{\hat{\tilde{u}}}_i\tilde{\hat{\tilde{u}}}_j)$, and $N_{ij} = B_{ij} - \widehat{A_{ij}}$.

An issue that requires some attention is the necessity to model separately the trace of the SGS stresses τ_{kk}. Yoshizawa (1986), Moin *et al.* (1991) and Speziale *et al.* (1988) proposed a separate model for this term. Erlebacher *et al.* (1992) conjectured that, for turbulent Mach numbers $M_t < 0.4$ this term is negligible; their DNS of isotropic turbulence confirm this conjecture. Zang *et al.* (1992) confirmed these results *a posteriori*: they ran calculations with $0 \le C_I \le 0.066$ (the latter value is 10 times higher than that predicted by the theory) and observed little difference in the results.

Comte and Lesieur (1998) proposed incorporating this term into a modified pressure $\mathcal{P}$. This leads to the presence of an additional term in the equation of state, which takes the

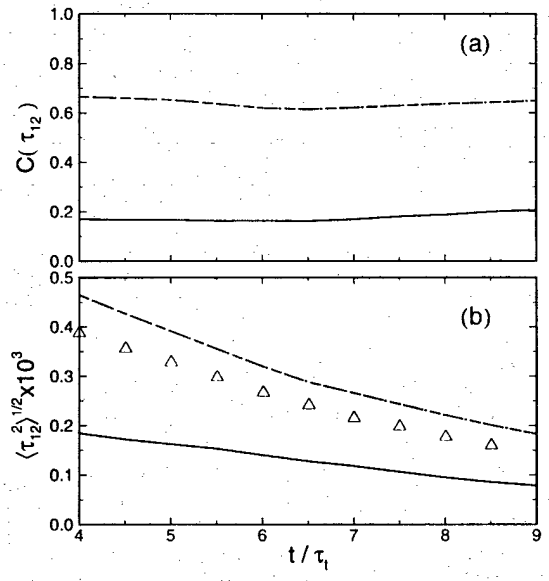

Figure 3: *A priori* comparison of the off-diagonal SGS stresses τ_{12}. (a) Correlation coefficient and (b) non-dimensional rms magnitude. —— Eddy-viscosity model DEV (16–17); --- two-coefficient mixed model DMM (18–19) and one-coefficient mixed model DMM-1 (21–22); △ DNS.

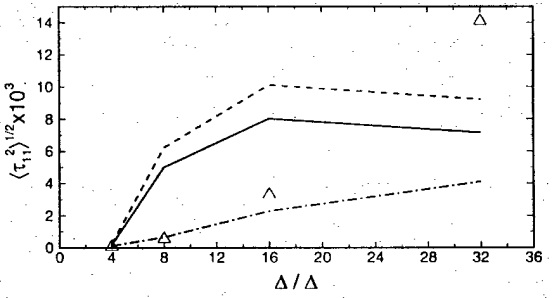

Figure 4: Non-dimensional rms magnitude of τ_{11} versus filter-width at $t/\tau_t = 6.5$. —— Eddy-viscosity model DEV (16–17); --- two-coefficient mixed model DMM (18–19); —·— one-coefficient mixed model DMM-1 (21–22); △ DNS.

(near 0.2), while much improved results are obtained with the mixed models. Note that the correlation coefficient for DMM and DMM-1 overlap in the figure. Figure 3b shows the rms of τ_{12}. DEV under-predicts the rms magnitude of the exact term, while DMM and DMM-1 slightly over-predict it.

The coefficient C_s remained nearly constant at a value of 0.15 throughout the calculation, consistent with the theoretical arguments (Yoshizawa, 1986). The coefficient of the SGS energy, C_I, on the other hand, has a value three times higher than predicted by the theory, consistent with the results of Moin *et al.* (1991).

Figure 4 shows the rms magnitude of τ_{11} *vs.* the filter-width, at time $t/\tau_t = 6.5$. Consistent with the results shown above for $\overline{\Delta}/\Delta = 8$, the one-coefficient mixed model DMM gives the most accurate predictions. For very small filter widths ($\overline{\Delta}/\Delta = 2$), all the models are accurate, reflecting the capability of dynamic models to turn off the model contribution when the grid becomes sufficiently fine to resolve all the turbulent structures (models with constants assigned *a priori*, such as the Smagorinsky (1963) model, do not have this characteristic). For intermediate filter-widths, up to $\overline{\Delta}/\Delta = 16$, the best prediction is given by the

where

$$I = -\overline{\Delta}^2\widehat{\overline{\rho}}\,|\widetilde{S}|\frac{\partial\widetilde{T}}{\partial x_j} + \overline{\Delta}^2\overline{\rho}\,\widehat{|S|\frac{\partial T}{\partial x_j}}. \qquad \lambda_j = \left(\widehat{\overline{\rho u_j}\,\overline{\rho T}}/\widehat{\overline{\rho}}\right) - \widehat{\overline{\rho u_j}}\,\widehat{\overline{\rho T}}/\widehat{\overline{\rho}} \tag{25}$$

A mixed model of the form

$$Q_j = -C\frac{\overline{\Delta}^2\overline{\rho}|\widetilde{S}|}{Pr_T}\frac{\partial\widetilde{T}}{\partial x_j} + \overline{\rho}\left(\widetilde{\widetilde{u}_j\widetilde{T}} - \widetilde{\widetilde{u}}_j\widetilde{\widetilde{T}}\right) \tag{26}$$

was proposed by Speziale *et al.* (1988). The model coefficients C and Pr_T can again be assigned, or adjusted dynamically according to (19) and

$$Pr_T = C\frac{\langle T_k T_k\rangle}{\langle K_j T_j\rangle - \langle V_j T_j\rangle}, \tag{27}$$

with

$$V_j = \widehat{\overline{\rho}}\left(\widehat{\widetilde{u}_j\widetilde{T}} - \widehat{\widetilde{u}}_j\widehat{\widetilde{T}}\right) - \overline{\rho}\left(\widehat{\widetilde{u}_j\widetilde{T}} - \widetilde{\widetilde{u}}_j\widetilde{\widetilde{T}}\right). \tag{28}$$

Figure 6a shows the correlation coefficient for the three models described above. Both eddy viscosity models overlap on the plot giving a poor correlation factor, roughly 0.2, whereas the mixed model gives a correlation above 0.6. Both eddy viscosity models underpredict the rms of the exact Q_j, shown in Fig. 6b, while the mixed model is more accurate. The mixed model maintains accuracy for all filter-widths $\overline{\Delta}/\Delta \leq 16$ (Fig. 7).

5.2 SGS viscous dissipation

The other term in the enthalpy or internal energy equations that was found to be significant in the present flow is the viscous dissipation ϵ_v. In this section, the three models proposed by Vreman *et al.* (1995b) are tested:

$$\epsilon_v^{(1)} = C_{v1}\left(\widetilde{\widetilde{\sigma}_{ij}\widetilde{S}_{ij}} - \widetilde{\widetilde{\sigma}}_{ij}\widetilde{\widetilde{S}}_{ij}\right); \tag{29}$$

$$\epsilon_v^{(2)} = C_{v2}\overline{\rho}\,\widetilde{q}^3/\overline{\Delta}, \qquad \widetilde{q}^2 \sim \overline{\Delta}^2|\widetilde{S}|^2; \tag{30}$$

$$\epsilon_v^{(3)} = C_{v3}\overline{\rho}\,\widetilde{q}^3/\overline{\Delta}, \qquad \widetilde{q}^2 \sim \widetilde{\widetilde{u}_k\widetilde{u}_k} - \widetilde{\widetilde{u}}_k\widetilde{\widetilde{u}}_k. \tag{31}$$

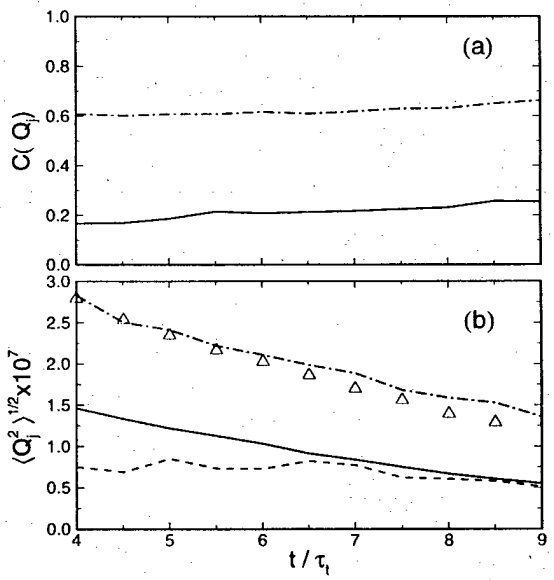

Figure 6: *A priori* comparison of the SGS heat flux Q_j. (a) Correlation coefficient and (b) non-dimensional rms magnitude. —— Eddy-diffusivity model (23), $Pr_T = 0.7$; --- eddy diffusivity model (23). Prandtl number adjusted according to (24); —·— mixed model (26-27); △ DNS.

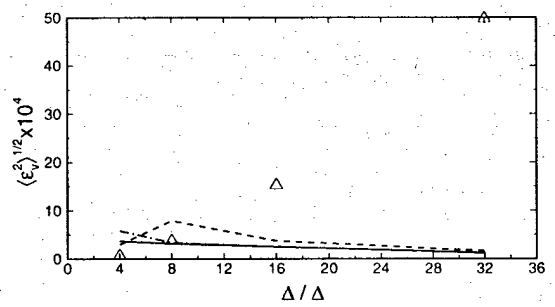

Figure 9: Non-dimensional rms magnitude of ϵ_v versus filter width at $t/\tau_t = 6.5$. —— Scale similar model (33); --- Dynamic model (34); —·— Dynamic model (35); △ DNS.

Figure 8a shows the correlation coefficient for the three models. All models give a correlation coefficient above 0.7. The use of a velocity scale obtained from the scale-similar assumption, however, results in improved prediction of the rms magnitude; using $q \sim \overline{\Delta}|\widetilde{S}|$ yields a significant over-prediction of the rms. The values of the coefficients obtained from the dynamic adjustment in this flow are significantly lower than those obtained in the mixing layer by Vreman *et al.* (1995b). For the particular filter-width shown, we obtained $C_1 = 2.4$, and $C_2 = 0.03$, while C_3 increased monotonically in time from 0.25 to 0.4. The fact that with these values the first and third models match the rms magnitude of the exact term indicates a lack of universality of these constants. Dynamic adjustment of the model coefficient appears to be beneficial for this term.

The modeling of the viscous dissipation is more sensitive than the other terms to the filter width. The prediction accuracy deteriorates with increasing filter-width, and in this case even for $\overline{\Delta}/\Delta = 16$ none of the models is particularly accurate (Fig. 9).

5.3 SGS turbulent diffusion

The SGS turbulent diffusion $\partial \mathcal{J}_j / \partial x_j$ appears in the total energy equation (6). Comte and Lesieur (1998) did not model this term explicitly, but added it to the SGS heat flux by using an eddy-diffusivity model to parameterize

$$-\left(\widetilde{\rho E u_j} + \widetilde{p u_j}\right) - \left(\overline{\rho}\,\widetilde{E}\widetilde{u}_j + \overline{p}\widetilde{u}_j\right) = \gamma \overline{\rho}\left(\widetilde{u_j T} - \widetilde{u}_j \widetilde{T}\right) + \mathcal{J}_j \simeq -\frac{\nu_T}{\overline{P}_{rT}} \frac{\partial \widetilde{T}}{\partial x_j}; \tag{36}$$

with this model, however, the SGS turbulent diffusion $\mathcal{J}_j$, which depends mostly on the unresolved velocity fluctuations, is modeled in terms of the temperature gradient. In an isothermal flow, $\mathcal{J}_j$ may be non-zero, and even if the temperature is not constant, there is no reason to couple a term due to mechanical energy gradients to the temperature. A model of the form (36) effectively neglects $\mathcal{J}_j$.

The only attempt to model the SGS turbulent diffusion was that by Knight *et al.* (1998). They argue that $\widetilde{u}_i \simeq \widetilde{\widetilde{u}}_i$ and propose a model of the form

$$\mathcal{J}_j \simeq \widetilde{u}_k \tau_{jk}. \tag{37}$$

A dynamic scale-similar model can be obtained using the generalized central moments (Germano, 1992):

$$\tau(u_i, u_j) = \overline{\rho}\left[\widetilde{u_i u_j} - \widetilde{u}_i \widetilde{u}_j\right] \tag{38}$$

$$\tau(u_i, u_j, u_k) = \overline{\rho}\,\widetilde{u_i u_j u_k} - \widetilde{u}_i \tau(u_j, u_k) - \widetilde{u}_j \tau(u_i, u_k) - \widetilde{u}_k \tau(u_i, u_j) - \overline{\rho}\,\widetilde{u}_i \widetilde{u}_j \widetilde{u}_k. \tag{39}$$

Using this notation the turbulent diffusion term can be written as

$$2\mathcal{J}_j = \tau(u_j, u_k, u_k) + 2\widetilde{u}_k \tau(u_j, u_k). \tag{40}$$

since $\tau(u_j, u_k) = \tau_{jk}$. Using this formalism, scale-similar models can be derived by approximating the quadratic terms using the filtered velocities $\widetilde{u}_i$ to replace the velocities u_i; for

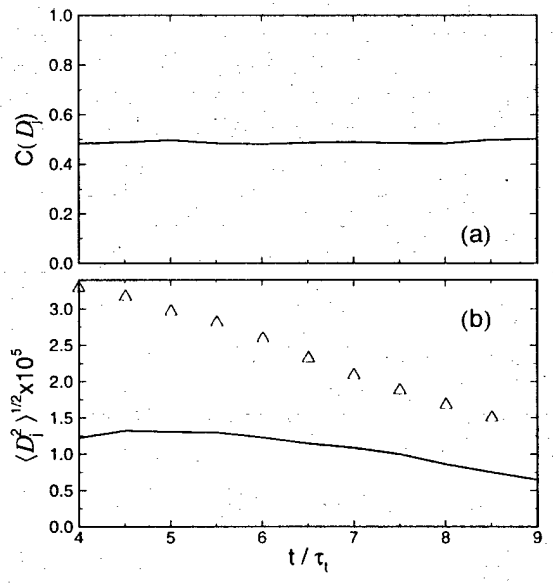

Figure 11: *A priori* comparison of the SGS viscous diffusion $\mathcal{D}_j$. (a) Correlation coefficient and (b) non-dimensional rms magnitude. —— scale-similar model; △ DNS.

rms magnitude of $\mathcal{J}_j$ (Fig. 10b). When the one-coefficient, scale-similar model is used this over-prediction is significantly reduced. Both models perform equally well for $\overline{\Delta}/\Delta \leq 16$, while neither is accurate for $\overline{\Delta}/\Delta = 32$.

5.4 SGS viscous diffusion

The SGS viscous diffusion $\partial \mathcal{D}_j/\partial x_j$ is the smallest of the terms in the total energy equation, and is about 5% of the divergence of Q_j. No model for this term has been proposed in the literature to date. One possibility is to parameterize it using a scale-similar model of the

form

$$\mathcal{D}_j = C_{\mathcal{D}}(\widetilde{\bar{\sigma}_{ij}\bar{u}_i} - \tilde{\bar{\sigma}}_{ij}\tilde{\bar{u}}_i). \tag{48}$$

in which the coefficient can be obtained from

$$C_{\mathcal{D}} = \frac{\left\langle \left[\widetilde{\frac{\overline{\rho\sigma}_{ij}\overline{\rho u_i}}{\bar{\rho}^2}} - \frac{\widetilde{\overline{\rho\sigma}_{ij}}\,\widetilde{\overline{\rho u_i}}}{\tilde{\bar{\rho}}^2} \right] \mathcal{R}_j \right\rangle}{\langle \mathcal{R}_k \mathcal{R}_k \rangle}. \tag{49}$$

where

$$\mathcal{R}_l = \left(\widetilde{\tilde{\bar{\sigma}}_{lk}\tilde{\bar{u}}_k} - \tilde{\tilde{\bar{\sigma}}}_{lk}\tilde{\tilde{\bar{u}}}_k \right) - \left(\widetilde{\bar{\sigma}_{lk}\bar{u}_k} - \tilde{\bar{\sigma}}_{lk}\tilde{\bar{u}}_k \right). \tag{50}$$

As can be seen from Fig. 11, this model gives a poor correlation and poor agreement for the prediction of the rms magnitude. However, since the viscous diffusion is relatively small, its contribution to the total energy spectrum does not go to the inertial range, but rather to the decaying range. In this situation the accuracy of the model is degraded, as shown by Meneveau and Lund (1997). Thus, the scale-similar approach may still give good predictions when this term is significant. In this particular flow, the error given by the model (or by not using a model) may be tolerable given the small contribution that the term gives to the energy budget.

6 Conclusions

Several mixed and eddy-viscosity models for the momentum and energy equations have been tested. The velocity, pressure, density and temperature fields obtained from the DNS of homogeneous isotropic turbulence at $Re_\lambda = 50$, $M_t = 0.52$ were filtered and the unclosed terms in the momentum, internal energy and total energy equations were computed.

In the momentum equation, mixed models were found to give better prediction, in terms of both correlation and *rms* amplitude, than the pure eddy-viscosity models. The dynamic adjustment of the model coefficient was beneficial, as already observed by Moin *et al.* (1991).

coefficients in the viscous range of turbulence. *Phys. Fluids* **9**, 3932-3934.

Moin, P., Squires, K. D., Cabot, W. H., and Lee, S. (1991). A dynamic subgrid scale model for compressible turbulence and scalar transport. *Phys. Fluids A* **3**, 2746-2757.

Normand, X., and Lesieur, M. (1992). Direct and large-eddy simulation of laminar breakdown in high speed axisymmetric boundary layers. *Theoret. Comput. Fluid Dyn.* **3**, 231-252.

Ristorcelli, J.R., and Blaisdell, G.A. (1997). Consistent initial conditions for the DNS of compressible turbulence. *Phys. Fluids*, **9**, 1-6.

Smagorinsky, J. (1963). General Circulation Experiments with the Primitive Equations. I. The Basic Experiment. *Monthly Weather Review* **91**, 99-164.

Speziale, C.G., Erlebacher, G., Zang, T.A., and Hussaini, M.Y. (1988) The subgrid scale modeling of compressible turbulence. *Phys. Fluids A* **31**, 940-942.

Vreman, B., Geurts, B., and Kuerten, H. (1995a). A priori tests of large eddy simulation of the compressible mixing layer. *J. Eng. Math.* **29**, 299-327.

Vreman, B., Geurts, B., and Kuerten, H. (1995b). Subgrid-modeling in LES of compressible flow. *Applied Sci. Res.* **54**, 191-203.

Yoshizawa, A. (1986). Statistical theory for compressible turbulent shear flows, with the application to subgrid modeling. *Phys. Fluids A* **29**, 2152-2164.

Zang, T. A., Dahlburg, R. B., and Dahlburg, J. P. (1992). Direct and large-eddy simulations of three-dimensional compressible Navier-Stokes turbulence. *Phys. Fluids A* **4**, 127-140.